Revelation of pivotal genes pertinent to Alzheimer's pathogenesis: A methodical evaluation of 32 GEO datasets

Hema Sree G N S
M. S. Ramaiah University of Applied Sciences
Saraswathy Ganesan Rajalekshmi (saraswathypradish@gmail.com)
M. S. Ramaiah University of Applied Sciences
Raghunadha R Burri
Dr. Reddy's Laboratories

Research Article

Keywords: BDNF, SST, SERPINA3, RTN3, RGS4

Posted Date: May 20th, 2021

DOI: https://doi.org/10.21203/rs.3.rs-533893/v1

Abstract

Background: Alzheimer's Disease (AD), a dreadful neurodegenerative disorder that affects cognitive and behavioral functions in geriatric population, is characterized by the presence of amyloid deposits and neurofibrillary tangles in hippocampus and cortex regions of the BRAIN. The 2018 World Alzheimer's Report exemplified a global prevalence of 50 million AD cases and forecasted a threefold rise upto 2 trillion by 2050. Although, there exist numerous genetic association studies pertinent to ad in different ethnicities, yet, critical genetic factors and signaling pathways underlying its pathogenesis still remain ambiguous. This study was aimed to collate and analyze the genetic data retrieved from 32 Gene Expression Omnibus (GEO) datasets belonging to diverse ethnic cohorts in order to identify overlapping Differentially Expressed Genes (DEGs). Stringent selection criteria were framed to shortlist appropriate datasets based on FDR p-value, log FC and relevant details on expression of both upregulated and downregulated DEGs from the same dataset.

Results: Among the 32 datasets, only 6 datasets satisfied the selection criteria. Geo2R tool was SUBSEQUENTLY employed to retrieve significant DEGs. Nine common DEGs viz. SLC5A3, BDNF, SST, SERPINA3, RTN3, RGS4, NPTX, ENC1 and CRYM WERE found in more than 60% of the selected datasets. These DEGs were later subjected to Protein-Protein Interaction analysis with 18 Literature Derived Genes specific to AD.

Conclusion: Among the nine common DEGs, BDNF, SST, SERPINA3 (AACT), RTN3 and RGS4 exhibited significant interactions with crucial proteins like BACE1, GRIN2B, APP, APOE, COMT, PSEN1, INS, NEP and MAPT. Functional enrichment analysis revealed involvement of these genes in trans-synaptic signalling, chemical transmission, PI3K pathway, receptor ligand activity, G-protein signalling etc. these processes are interlinked with AD pathways.

Introduction

Alzheimer's Disease (AD), a progressive irreversible neurodegenerative disorder, affecting the elderly IS characterized by dementia and disruptive cognitive functioning. It represents one of the highest unmet medical requirements. World Alzheimer's Report that exemplified a global prevalence of 50 million in 2018 also forecasted a threefold rise of AD cases up to 2 trillion by 2050 [1]. Around 1.21 lakh deaths due to Alzheimer's dementia were reported in 2019. In the recent past, during the Corona Virus Disease 19 (COVID-19) pandemic, fatality rates amongst AD patients had mounted to 145% [2]. Alzheimer's and Related Disorders Society of India (ARDSI) foretold a huge burden of 6.35 million AD cases across India by the year 2025 [3].

Till date, the U.S. Food and Drug Administration (US-FDA) has approved only four anti AD drugs belonging to the following categories like i) Cholinesterase Inhibitors: Donepezil, Rivastigmine and Galantamine; and ii) N-Methyl D-Aspartate receptor antagonist: Memantine [8]. The aforementioned AD drug therapy is oriented towards meagre symptomatic relief and offers modest clinical effect.

Looking into the pathophysiology, neuropathological evidences state that AD is characterized by presence of Amyloid Beta plaques (Aβ) and Neurofibrillary Tangles (NFT) in hippocampus and cortex regions. Though there were various complex pathophysiological theories explaining the role of numerous genes and proteins in AD progression, major role is attributed to Presenilin 1 (PSEN1), Beta-Secretase 1 (BACE1), Amyloid Precursor Protein (APP) and Microtubule Associated Protein Tau (MAPT) proteins [4]. Disruption in regulatory activities like phosphorylation and dephosphorylation of these proteins result in AD progression. Notwithstanding the existence of countless genetic evaluations, inconsistencies among various ethnicities contribute to a lacuna in unravelling

crucial disease specific targets. This study was aimed to explore the major genetic alterations among various microarray datasets to retrieve common Differentially Expressed Genes (DEGs) among various ethnicities with the hypothesis that overlapping DEGs across different ethnicities might play a definitive role in AD pathogenesis.

Methodology

Selection of datasets:

Microarray datasets pertaining to Alzheimer's disease were retrieved from the Gene Expression Omnibus (GEO) database [5] using keywords: "Alzheimer's disease", "Familial Alzheimer's disease", "Sporadic Alzheimer's disease", "Early onset Alzheimer's disease" and "Late onset Alzheimer's disease". The datasets retrieved through the above search terms were screened through a set of inclusion and exclusion criteria.

Inclusion criteria:

Datasets satisfying all the following criteria were selected

- Datasets with controls and AD
- Datasets with expressional arrays
- Datasets describing the diagnostic criteria of AD
- Datasets studied in *"Homo sapiens"*
- Datasets with minimum of 2 samples in each category i.e., control and AD
- Datasets with blood/brain samples

Exclusion criteria:

Datasets with following criteria were excluded.

- Drug treated datasets.
- Methylation studies
- Datasets with nil diagnostic criteria
- Cell line studies
- Datasets from other organisms
- Datasets with no details about controls
- Mutation studies

Gene expression analysis:

The selected datasets were preprocessed, curated and analyzed individually for retrieval of Differentially Expressed Genes (DEGs) (both upregulated and downregulated) through Bioconductor package. The datasets which revealed DEGs with False Discovery Rate (FDR) p-value (adjusted p-value according to Benjamin-Hochberg method) <0.05 were selected. Later these datasets were subjected to four sets of filtering criteria based on FDR and log Fold Change (FC) viz., (i) FDR p-value <0.05 and log FC >2, (ii) FDR p-value < 0.05 and log FC >1.5, (iii) FDR p-value <0.05 and log FC >1 and (iv) FDR p-value <0.01 and log FC >1. Based on the above stringent filtering criteria, the datasets possessing following characteristics were included: (a) the datasets satisfying one of the above four

criteria, (b) the datasets those encompass both upregulated and downregulated DEGs and (c) 60% of the datasets showing aforementioned characteristics (a & b) should display higher degree of common DEGs.

Protein-Protein Interaction (PPI) analysis:

The common DEGs retrieved from the above step were subjected to PPI analysis with Literature Derived Genes (LDGs) (gathered from National Centre for Biotechnology Information (NCBI) [6]) pertinent to AD progression through Search Tool for the Retrieval of Interacting Genes/Proteins (STRING) database [7]. PPI network is visualized through cytoscape with proteins as nodes and interactions as edges. The proteins exhibiting significant interactions (70% confidence score) with LDGs were shortlisted and the nodes exhibiting node degree > 2 were selected as AD targets.

Functional Enrichment analysis:

The retrieved common DEGs were subjected to functional enrichment analysis to explore their involvement in signaling pathways and physiological functions associated with AD pathogenesis through ClueGO [8] in cytoscape.

Results

Selection of datasets:

Around 134 GEO datasets derived from studies performed on *"Homo sapiens"* were retrieved from NCBI, out of which 32 datasets were found to satisfy initial inclusion criteria. The details pertaining to 32 datasets were described in Table-1

Table-1 List of GEO datasets selected for the study

Dataset Accession Number	Pubmed reference	Number of Cases	Number of Controls	Genetic source	Genotyping platform	Genotyping method
GSE36980 [9]	23595620,	32	47	Brain (Hippocampus, frontal cortex and temporal cortex)	GPL6244	RT-PCR
GSE28146 [10]	21756998	22	8	Brain (CA1 hippocampal gray matter)	GPL570	microarray (Affymetrix HGU133 v2) hybridization
GSE4757 [11]	16242812	10	10	Brain entorhinal cortex	GPL570	Affymetrix U133A arrays
GSE4226 [12] [13]	16979800 19366883	14	14	Peripheral Blood Mononuclear Cells (PBMC)	GPL1211	QRT-PCR
GSE1297 [14]	14769913	22	9	Hippocampal	GPL96	Affymetrix GeneChip Expression Analysis
GSE110226 [15] [16]	29848382 30541599	7	6	lateral ventricular choroid plexus	GPL10379	Human Affymetrix GeneChip microarray
GSE93885 [17]	29050232	14	4	human olfactory bulb	GPL16686	Affymetrix Human Gene 2.0 ST
GSE97760 [18]	25079797	9	10	Peripheral blood	GPL16699	Agilent-039494 SurePrint G3 Human GE v2 8x60K Microarray 039381
GSE63060 [19]	26343147	145	104	Peripheral blood	GPL6947	Illumina HumanHT-12 V3.0 expression beadchip
GSE63061 [19]	26343147	139	134	Brain, muscle	GPL6947	Illumina

				and skin		Human HT-12 V3 Bead chip
GSE5281 [20][21][22][23]	17077275 18332434 29937276 18270320	87	71	entorhinal cortex, hippocampus, medial temporal gyrus, posterior cingulate, superior frontal gyrus, primary visual cortex	GPL570	Affymetrix U133 Plus 2.0 array
GSE6834 [24]	17343748	20	20	Temporal Cortex, Cerebellum	GPL4757	Ion Channel Splice Array
GSE12685 [25]	19295912	6	8	prefrontal cortices	GPL96	Affymetrix Human Genome U133A Array
GSE4227 [26][13]	18423940 19366883	16	18	Peripheral blood mononuclear cells	GPL1211	NIA Human MGC cDNA microarray
GSE4229 [13]	19366883	18	22	Peripheral blood mononuclear cells	GPL1211	NIA Human MGC cDNA microarray
GSE15222 [27]	19361613	176	187	Cortical	GPL2700	Sentrix HumanRef-8 Expression BeadChip
GSE18309 [28]	21669286	3	3	blood leukocytes	GPL570	Affymetrix Human Genome U133 Plus 2.0 Array
GSE16759 [29]	20126538	4	4	parietal lobe	GPL570	Affymetrix Human Genome U133 Plus 2.0 Array
GSE32645 [30]	23687122	3	3	Cortices	GPL4133	Whole Human Genome

						Microarray 4x44K G4112F
GSE26927 [31] [32]	22864814 25119539	11	7	Brain	GPL6255	Illumina humanRef-8 v2.0 expression beadchip
GSE61196 [33]	26573292	14	7	choroid plexus	GPL4133	Agilent-014850 Whole Human Genome Microarray 4x44K G4112F
GSE33000 [34]	25080494	310	157	Dorsolateral prefrontal cortex	GPL4372	Rosetta/Merck Human 44k 1.1 microarray
GSE37264 [35]	26484111	8	8	Brain	GPL5188	Affymetrix Human Exon 1.0 ST Array
GSE48350 [36] [37][38][39]	23273601 22824372 20838618 23999428	80	173	hippocampus, entorhinal cortex, superior frontal cortex, post-central gyrus	GPL570	Affymetrix Human Genome U133 Plus 2.0 Array
GSE132903 [40]	31256118	97	98	middle temporal gyrus	GPL10558	Illumina Human HT-12 v4 arrays
GSE131617 [41]	26126179	175	38	entorinal, temporal and frontal cortices	GPL5175	Affymetrix Human Exon 1.0 ST Array
GSE122063 [42]	30990880	12	10	frontal cortex	GPL16699	Agilent-039494 SurePrint G3 Human GE v2 8x60K Microarray 039381
GSE26972 [43]	22628224	3	3	human entorhinal	GPL5188	Affymetrix Human Exon

				cortex		1.0 ST Array
GSE37263 [44]	19937809	8	8	BA22	GPL5175	Affymetrix Human Exon 1.0 ST Array
GSE118553 [45]	31063847	85	27	entorhinal cortex, temporal cortex, frontal cortex, cerebellum	GPL10558	Illumina HumanHT-12 V4.0 expression beadchip
GSE29378 [46]	23705665	31	32	Hippocampus	GPL6947	Illumina HumanHT-12 V3.0 expression beadchip
GSE13214 [47]	23144955	52	40	Hippocampus, Cortex	GPL1930	Homo sapiens 4.8K 02-01 amplified cDNA

(i) FDR p-value <0.05 and log FC >2:

Out of the 16 qualified datasets, 5 datasets possessing upregulated DEGs and 4 datasets with downregulated DEGs (Fig. 2) satisfied this criterion (Table 2 & 3). Nevertheless, the upregulated DEGs of two datasets of the five displayed overlapping genes while, the downregulated DEGs of the shortlisted datasets did not show common genes. Therefore, this criterion was rejected.

(ii) FDR p-value < 0.05 and log FC > 1.5:

Among the 16 datasets, only 6 datasets were found to meet this criterion (Table 2 & 3). Common DEGs were found in datasets which accounts for 50% and thus did not meet the characteristic ‘c’ mentioned in the methodology section (Fig. 3). Thus, this criterion was also rejected

(iii) FDR p-value < 0.05 and log FC >1:

Among the 16 datasets, this criterion was met by 9 datasets with upregulated DEGs and 8 datasets with downregulated DEGs (Table 2 & 3). Also, the number of datasets were not equal and the common DEGs were not seen in 60% of the datasets. Therefore, this criterion was rejected.

(iv) FDR p-value < 0.01 and log FC > 1

Among the 16 datasets, this criterion was met by 6 datasets containing both upregulated and downregulated DEGs (Table 2 & 3). Common upregulated and downregulated DEGs were found in 4 datasets which accounts for more than 60%. Hence, this criterion was selected to retrieve the DEGs for PPI and functional enrichment analysis. Among upregulated DEGs, Solute Carrier Family 5 Member 3 (SLC5A3) and Serpin Family A Member 3 (SERPINA3)

were found to be common in 4 datasets. Among downregulated DEGs, Somatostatin (SST), Regulator of G protein signalling 4 (RGS4), Crystallin Mu (CRYM), Neuronal Pentraxin 2 (NPTX2), Reticulon 3 (RTN3), Brain Derived Neurotrophic Factor (BDNF) and Ectodermal-Neural Cortex 1 (ENC1) genes were found to be common in 4 datasets (Fig. 4). These genes were selected for further PPI Analysis with LDGs.

Table-2 Number of DEGs obtained through filtering criteria

Datasets Accession Number	Number of DEGs
FDR p-value<0.05 and log FC>2	
Upregulated	
GSE110226	22
GSE15222	18
GSE48350	6
GSE5281	13
GSE97760	1463
Downregulated	
GSE110226	6
GSE48350	1
GSE5281	27
GSE97760	1307
FDR p-value < 0.05 and log FC > 1.5	
Upregulated	
GSE110226	33
GSE122063	129
GSE15222	32
GSE48350	6
GSE5281	123
GSE97760	1998
Downregulated	
GSE110226	15
GSE122063	111
GSE15222	5
GSE48350	3
GSE5281	273
GSE97760	1235
FDR p-value < 0.05 and log FC >1	
Upregulated	
GSE110226	99
GSE131617	8
GSE132903	2
GSE15222	144
GSE29378	7
GSE48350	11
GSE5281	885
GSE63061	1
GSE97760	4231
Downregulated	
GSE110226	35
GSE122063	663
GSE132903	38
GSE15222	48
GSE48350	9

GSE5281	1507
GSE63060	4
GSE97760	2543
FDR p-value < 0.01 and log FC > 1	
Upregulated	
GSE122063	386
GSE132903	2
GSE15222	111
GSE48350	11
GSE5281	834
GSE97760	2987
Downregulated	
GSE122063	653
GSE132903	28
GSE15222	45
GSE48350	9
GSE5281	1449
GSE97760	1580

Table-3 List of common DEGs obtained through filtering criteria

Datasets no	Common DEGs
FDR p-value<0.05 and log FC>2	
Upregulated	
GSE48350 & GSE97760	SLC25A46, ZNF621, XIST and ANKIB1
GSE5281 & GSE97760	RBM33, NEAT1 and MALAT1
GSE110226 & GSE97760	IL1RL1 and SERPINA3
Upregulated	
GSE110226, GSE122063 and GSE97760	SERPINA3 & IL1RL1
GSE122063, GSE5281 and GSE97760	NEAT1
GSE15222, GSE5281 and GSE97760	SLC5A3
GSE122063, GSE48350 and GSE97760	XIST
GSE5281 and GSE97760	RGPD5, JPX, ZMYM5, CCDC144A, SNRNP48, ZBED6, SKI, ANKRD36, MECOM, ZDHHC21, UBE3A, RAB18, RBM25, RGPD6, RBM33, RRBP1, SEPT7, GOLIM4, ANKRD12, ZC3H11A, MALAT1 and RANBP2
GSE122063 and GSE97760	CCDC66, HMBOX1, IL18R1 and GON4L
GSE48350 and GSE97760	SLC25A46 and ANKIB1
GSE15222 and GSE97760	RAD51C and F8
GSE122063 and GSE5281	SOCS3 and SNX31
Downregulated	
GSE122063, GSE15222	RGS4 and SST

and GSE5281	
GSE110226 and GSE97760	SFRP2, TCF21 and HMGCLL1
GSE110226 and GSE122063	CTXN3
GSE5281 and GSE97760	TSTA3, DUSP4, DCTN1, SLIT3, SEZ6L2, CALY, SNCA, BLVRB, INA, PTPRF, CPNE6, ATP6 and V1G2
GSE15222 and GSE97760	NELL1
GSE122063 and GSE97760	GPR88, STMN1, RPH3A, DNAH2 and NRIP3
GSE122063 and GSE5281	RTN1, BDNF, VSNL1, NMNAT2, RPS4Y1, PTPN3 and MAL2
GSE122063 and GSE5281	HSPB3
FDR p-value < 0.05 and log FC >1	
Upregulated	
GSE132903, GSE15222, GSE5281 and GSE97760	SLC5A3
GSE110226, GSE29378 and GSE97760	SERPINA3
GSE15222, GSE5281 and GSE97760	RHOQ and IL6ST
GSE131617, GSE5281 and GSE97760	PPA2
GSE110226 and GSE97760	IL1RL1, IL4R, IL18R1 and C1orf21
GSE110226 and	SOCS3, MT2A, C10orf54, FBXO32, BACE2, GALNT15 and SLCO4A1

GSE5281	
GSE110226 and GSE15222	GPRC5A
GSE5281 and GSE97760	HD9, IPW, QKI IL6R, PTPN2, UBE2W, AHNAK, JPX, CASC4, RDX, FAM161A, ZMYM5, SET, FAM120A, SNORA18, BDP1, C5orf56, PPFIBP1, YTHDC2, ELF1, CCDC144A, TAF1D, ZNF713, SNRNP48, SNORD107, SNORD50B, LRRFIP1, ELK4, GRAMD1C, SNORD61, LMO7, SAMHD1, PTBP3, TRIM4, CXCL2, TNPO1, CDK13, ZFP36L1, SEPT8, STAG1, SKI, TBL1XR1, SNORA1, ANKRD36, CPEB4, MKL2, MBTD1, HCG18, ZNF160, MECOM, PDE4DIP, ZDHHC21, CBX3, TFEB, SKIL, TLE4, IFNAR2, KCNJ16, SLC4A4, KTN1, SAT1, ABLIM1, ZNF280D, RBMS1, LZTS2, LPP, ATRX, MACF1, PCMTD2, C5orf24, TPP2, SFPQ, ZSCAN30, STAG2, RBM33, RAPH1, SOS2, SNORA40, WHAMMP2, NEAT1, ZNF566, PIK3C2A, NOTCH2NL, LEF1, NEK1, MYH11, SNORD5, ITPR2, SEPT7, PTAR1, FXR1, TUBE1, SGPP2, USP6, FAM198B, ZBTB1, SNORA8, TP53INP1, SNORD84, FAM185A, NFATC2, ANKRD12, MKRN3, RBMX, TCF7L2, ZNF800, MALAT1, SREK1, GKAP1, TRIM59, UHRF1, WNK1, TRPS1, MIB1, STK17B, SCARNA17, TOB1, MDM4, CCDC88A, DCAF8, ZNF638, ANKRD36B, USP47, SYCP3, CDC14A, TRA2B, FAM98B, PPM1K, BDH2, KDM5A, RGPD5, ANKRD10-IT1, SNORD116-4, NKTR, FRYL, SPAG9, UBE2D3, SMCHD1, FAM107B, SCFD1, ZBED6, RNPC3, ZFAND6, SMG1, ALS2, PTPRC, PNISR, NUCKS1, TSIX, CNTLN, BRD7, NSUN6, PIGY, CELF2, LUC7L3, DDX59, UBE2Z, PLGLB1, ANKRD13A, RUFY3, DDX39B, UBE3A, RAB18, LOC100133089, RBM25, CCDC7, BHLHE41, SRRM2, RGPD6, PTEN, AGFG1, RASSF3, AASDH, KDELC2, DACH1, REST, FNIP1, KIF5B, PRKD3, IFT80, C11orf58, PPIG, ZNF138, PARP11, CARD6, MORF4L2, TMTC3, SLC44A1, PYHIN1, SNORA32, RRBP1, NEDD1, EPC1, PRPF38B, C16orf52, MIAT, CCNC, DIS3L2, SEPT7P2, CLTC, RPS16P5, SREK1IP1, PPP1R12B, NSF, SP100, CAPRIN1, CNTRL, GNAQ, ESF1, TNFAIP8, LOC100129447, FGFR1OP2, EIF3C, SCAMP1, GOLIM4, ZEB2, CADM1, PAIP2B, YLPM1, ZC3H11A, TTN, HBS1L, RHOBTB3, ZNF638-IT1, VPS13C, RANBP2, MARVELD2, C3orf38, SCAF11, WHAMMP3, FCHO2 and TOP1
GSE15222 and GSE97760	LDHAL6A, FANCC, ARMCX3, SLC26A2, PCDHGB3, TBC1D23, PSMA1, F8, GFM2, DDX6, ZNF326, IL7, FGF5, CD1C, SYNE2, PBRM1, RAD51C, LONRF3, RNF13, TIFA and FANCB
GSE48350 and GSE97760	SLC25A46, ANKIB1, XIST and ZNF621
GSE29378 and GSE97760	RGS1
GSE15222 and GSE5281	XAF1, SRGAP1, PATJ, YPEL2, GBP2, LATS2, MRGPRF, ITPRIPL2, GRTP1, MKNK2, ZIC1 and ANGPT2
GSE48350 and GSE5281	CXCR4
GSE29378 and	CD44 and CD163

GSE5281	
GSE132903 and GSE5281	GFAP
GSE15222 and GSE48350	C4B and LTF
Downregulated	
GSE110226, GSE122063, GSE5281 and GSE97760	HMGCLL1
GSE122063, GSE15222, GSE5281 and GSE97760	NELL1
GSE122063, GSE15222, GSE48350 and GSE5281	SST
GSE122063, GSE132903, GSE15222 and GSE5281	RGS4, ENC1, PCSK1, CRYM and NPTX2
GSE110226, GSE122063 and GSE97760	HDC
GSE15222, GSE5281 and GSE97760	ROBO2
GSE122063, GSE5281 and GSE97760	PAX7, TSPAN7, STMN1, WBSCR17, MAP7D2, SULT4A1, INA, NRIP3, DOCK3, IGF1, REEP1, CGREF1, ICA1, SPHKAP, LAMB1 and ZDHHC23
GSE122063, GSE15222 and GSE97760	TAC3
GSE132903, GSE15222	SERPIN1

and GSE5281	
GSE122063, GSE15222 and GSE5281	ADCYAP1, ZBBX, NEUROD6, GRP, SLC30A3, CARTPT, CRH and SERTM1
GSE122063, GSE48350 and GSE5281	ABCC12, CALB1 and MIR7-3HG
GSE122063, GSE132903 and GSE5281	RTN1, PRKCB, NELL2, NEFM, HPRT1, DYNC1I1, PARM1, GABRA1, CHGB, GABRG2, RGS7 and SYT1
GSE122063, GSE132903 and GSE15222	VGF and NECAB1
GSE110226 and GSE97760	SFRP2, TCF21, ADAMTSL1, EGFEM1P and IGSF1
GSE110226 and GSE5281	LYRM9
GSE110226 and GSE122063	CTXN3 and NPY2R
GSE5281 and GSE97760	ATXN10, DUSP4, SSU72, KIAA1324, SEZ6, SYTL5, DCTN1, TALDO1, FIS1, GPX4, PTP4A3, SNCA, HN1, AP2S1, KCTD2, MCAT, BLVRB, DPP6, NCAM2, ATP6V0C, KCNG3, SYNE1, SPTBN2, ATRNL1, ATP2B3, PTGER3, ATP6V0D1, DNAJA4, LMF1, SGIP1, CROT, ANKS1B, ANK2, SLIT3, SEZ6L2, RNF187, ANKRD54, CALY, TSPAN5, CSRNP3, MFSD2B, HGD, DAB2IP, CX3CL1, RANBP10, AHNAK2, DPCD, PAK1, NOC4L, UBL7, HAGH, ASPSCR1, TRAPPC5, CNKSR2, LOC729870, DCAF6, CD99L2, PTPRF, CPNE6, RNF24, TBC1D7, NAV3, ATP6V1G2, TMEM59L, SLC24A3, MLXIP, TSTA3, FOLH1, SPTAN1, TCEA2, AP2M1, SMOX, FHL2, ASCC2, PRDX5, FKBP1B, HYDIN, AP3B2, PDE1A, FAM131A, TMEM158, NFIB, UMODL1, MEG3 and GCAT
GSE15222 and GSE97760	DGKB and CORT
GSE122063 and GSE97760	GLT1D1, NOS2, XK, FAM182B, PTPN5, RTN4RL1, NECAB2, PRRT1, LOC284395, SSX3, KIAA1045, NKX2-3, PVALB, CHRFAM7A, KIAA1239, GSG1, ADCY2, FAM178B, GLP2R, LOC100289580, WNK2, GYG2P1, LRRC38, DDAH1, TBXA2R, RET, LOC100507534, ZSCAN1, OCA2, HAPLN1, INSL3, ENTPD3, KATNB1, RPL13AP17, NAALADL2, ST7-AS1, NPPA, SLC7A4, PCDH11X, RPH3A, CASQ1, ODZ3, NGEF, KIAA1644, LOC653550, MYO5B, PNMA5, LOC338797, KCNH2, TUBA3C, LOC100288814, LOC497256, DRGX, GPR88, CHRM2, PRKAR1B, FLJ32255, LOC100134259, SLC22A10 and PVRL3-AS1

GSE15222 and GSE5281	GABRA5, ANO3, AP1S1, SERINC3, ITFG1, ICAM5, PGM2L1, CCK, PLK2 and NCALD
GSE132903 and GSE5281	GLRB, ERICH3, TUBB2A and NSF
GSE122063 and GSE5281	GDA, MET, SERPINF1, LINC00460, ZNF385B, SYT13, LOC283484, SARS, CHRM1, CHRNB2, GPATCH2, KRT222, NMNAT2, UBE2N, ZCCHC12, GPR158, SDR16C5, FGF12, FPGT-TNNI3K, TAC1, RNF175, UBE2QL1, SYN2, ATL1, AMPH, MYT1L, NAP1L5, TAGLN3, C14orf79, UNC13A, SOSTDC1, SH3GL2, STMN2, MAP4, MDH1, STAT4, VSNL1, GPRASP2, EPHA5, TRIM37, FAR2, PCLO, SV2B, SVOP, PAK3, CDC42, CAMK1G, PPP1R2, NOP56, PTPRO, BSCL2, CIRBP, HS6ST3, PPP1R14C, SCG5, NPTXR, GLS2, GOLT1A, TASP1, ACOT7, RSPO2, ENO2, NEFL, CD200, RBM3, GAP43, ERC2, GNG2, PPM1E, RPS4Y1, TARBP1, SLC1A6, GNG3, NECAP1, GABRD, GLS, LINC00467, NRXN3, LY86-AS1, ATP8A2, MLLT11, BRWD1, PPM1J, RAB3C, UCHL1, WDR54, BDNF, DCLK1, PNMAL2, CITED1, NUDT18, RAB27B, SNAP25, GOLGA8A, HMP19, LOC100506124, SYCE1, CCKBR, TUBB3, COPG2IT1, RBP4, PPEF1, CACNG3, MICAL2, LOC100129973, PTPN3, PLD3, ATOH7, MAL2 and BEX5
GSE122063 and GSE15222	SCG2, VIP, KCNV1, TMEM155, NMU, HSPB3 and PCDH8
GSE122063 and GSE48350	SLC32A1
GSE122063 and GSE132903	CAP2
FDR p-value < 0.01 and log FC > 1	
Upregulated	
GSE132903, GSE15222, GSE5281 and GSE97760	SLC5A3 and SERPINA3
GSE15222, GSE5281 and GSE97760	RHOQ and IL6ST
GSE122063, GSE5281 and GSE97760	FAM107B, ZBED6, NEAT1, RRBP1 and TTN
GSE122063, GSE15222 and GSE5281	GBP2 and ANGPT2
GSE122063,	GFAP

GSE132903 and GSE5281	
GSE122063, GSE15222 and GSE48350	C4B and LTF
GSE5281 and GSE97760	USP47, CHD9, IPW, TRA2B, FAM98B, PPM1K, BDH2, KDM5A, QKI, RGPD5, ANKRD10-IT1, IL6R, SNORD116-4, NKTR, FRYL, PTPN2, AHNAK, UBE2W, JPX, RDX, FAM161A, ZMYM5, SET, FAM120A, SNORA18, BDP1, C5orf56, UBE2D3, YTHDC2, SMCHD1, CCDC144A, TAF1D, ZNF713, SNRNP48, SNORD107, RNPC3, SNORD50B, LRRFIP1, ELK4, ALS2, PTPRC, GRAMD1C, PNISR, SNORD61, LMO7, NUCKS1, CNTLN, SAMHD1, PTBP3, TRIM4, CXCL2, TNPO1, CDK13, ZFP36L1, STAG1, BRD7, SKI, TBL1XR1, SNORA1, ANKRD36, CPEB4, NSUN6, MKL2, PIGY, HCG18, ZNF160, CELF2, LUC7L3, MECOM, DDX59, UBE2Z, ZDHHC21, CBX3, ANKRD13A, TFEB, RUFY3, SKIL, UBE3A, TLE4, RAB18, LOC100133089, RBM25, KCNJ16, CCDC7, KTN1, RGPD6, SAT1, ABLIM1, ZNF280D, RBMS1, LPP, ATRX, MACF1, PCMTD2, AGFG1, RASSF3, AASDH, C5orf24, KDELC2, SFPQ, ZSCAN30, STAG2, RBM33, RAPH1, REST, FNIP1, KIF5B, SNORA40, PPIG, ZNF138, ZNF566, PIK3C2A, PARP11, NOTCH2NL, LEF1, MORF4L2, TMTC3, NEK1, SLC44A1, PYHIN1, SNORD5, NEDD1, EPC1, PRPF38B, C16orf52, MIAT, SEPT7, CCNC, DIS3L2, SEPT7P2, PTAR1, TUBE1, SREK1IP1, NSF, USP6, SP100, CAPRIN1, ZBTB1, CNTRL, SNORA8, TP53INP1, GNAQ, ESF1, TNFAIP8, SNORD84, FGFR1OP2, EIF3C, FAM185A, SCAMP1, GOLIM4, ZEB2, CADM1, ANKRD12, YLPM1, ZC3H11A, RBMX, HBS1L, ZNF800, RHOBTB3, MALAT1, SREK1, GKAP1, UHRF1, WNK1, VPS13C, TRPS1, RANBP2, C3orf38, SCAF11, VSIG10, WHAMMP3, FCHO2, MIB1, STK17B, SCARNA17, TOB1, MDM4, CCDC88A and DCAF8
GSE15222 and GSE97760	SLC26A2, FGF5, TBC1D23, PSMA1, PBRM1, RAD51C, F8, LONRF3, DDX6, ZNF326 and FANCB
GSE48350 and GSE97760	SLC25A46, XIST, ZNF621 and ANKIB1
GSE122063 and GSE97760	AHSA2, CHORDC1, EIF4G3, CCDC66, LOC100287765, Q5A5F0, SNORA75, MSR1, F13A1, WDR33, LOC100507645, ZNF620, IL18R1, SERPINA3, ZNF850, AFF1, GON4L, RUNX1, IL1RL1, LOC387895, CA5BP1, SNORA73A, CXCL12, RBM47, LRRC37A3, EFTUD1, LOC100129089, SPATA13 and PLAC8
GSE15222 and GSE5281	MRGPRF, ITPRIPL2, XAF1, GRTP1, MKNK2, SRGAP1, PATJ, YPEL2, ZIC1 and LATS2
GSE48350 and GSE5281	CXCR4
GSE122063 and GSE5281	CD44, HIGD1B, BACE2, PIEZO2, SOCS3, CEP104, EGFR, PDLIM4, ITPKB, RHOJ, PDE4DIP, VASP, COL27A1, MAFF, KCNE4, SCIN, MYO10, SNX31, ZFP36L2, EMP1, SLCO1A2, TNS1, SRGN, SLCO4A1, CD163, TBL1X, CXCL1, BCAS1, TNFRSF10B, FAM65C and LOC100131541
GSE122063	FOXJ1, MIA, S100A12, S100A4 and C21orf62

and GSE15222	
GSE122063 and GSE48350	C4A
Downregulated	
GSE122063, GSE15222, GSE48350 and GSE5281	SST and BDNF
GSE122063, GSE132903, GSE15222 and GSE5281	RGS4, CRYM, NPTX2, RTN3 and ENC1
GSE15222, GSE5281 and GSE97760	ROBO2
GSE122063, GSE5281 and GSE97760	IGF1, STMN1, REEP1, CGREF1, ICA1, SPHKAP, WBSCR17, MAP7D2, SULT4A1, LAMB1, ZDHHC23, NRIP3, HMGCLL1 and DOCK3
GSE122063, GSE15222 and GSE97760	TAC3
GSE122063, GSE15222 and GSE5281	ADCYAP1, CRH, ZBBX, NEUROD6, SLC30A3, NELL1, CARTPT and SERTM1
GSE122063, GSE48350 and GSE5281	ABCC12, CALB1 and MIR7-3HG
GSE122063, GSE132903 and GSE5281	RTN1, PRKCB, NELL2, GABRA1, CHGB, GABRG2, NEFM, RGS7, SYT1, HPRT1, DYNC1I1 and PARM1
GSE122063, GSE132903 and GSE15222	PCSK1, VGF and NECAB1
GSE5281 and GSE97760	NOC4L, ATXN10, DUSP4, SSU72, KIAA1324, SEZ6, UBL7, DCTN1, HAGH, ASPSCR1, FIS1, PTP4A3, SNCA, HN1, AP2S1, KCTD2, MCAT, CNKSR2, BLVRB, DCAF6, CD99L2, ATP6V0C, CPNE6, SYNE1, TBC1D7, NAV3, ATP6V1G2, TMEM59L, ATRNL1, MLXIP,

	LMF1, SPTAN1, SGIP1, CROT, SMOX, FHL2, ASCC2, SEZ6L2, CALY, FKBP1B, TSPAN5, FAM131A, TMEM158, DAB2IP, CX3CL1, MEG3, GCAT and DPCD
GSE15222 and GSE97760	CORT and DGKB
GSE122063 and GSE97760	XK, KATNB1, FAM182B, RPL13AP17, PTPN5, RTN4RL1, ST7-AS1, NPPA, PRRT1, PCDH11X, LOC284395, SSX3, KIAA1045, CASQ1, ODZ3, KIAA1644, NKX2-3, PVALB, CHRFAM7A, KIAA1239, GSG1, ADCY2, FAM178B, LOC100289580, WNK2, MYO5B, PNMA5, LOC338797, KCNH2, RET, LOC497256, LOC100507534, ZSCAN1, GPR88, CHRM2, PRKAR1B, FLJ32255, SLC22A10, PVRL3-AS1 and OCA2
GSE15222 and GSE5281	PGM2L1, GABRA5, ANO3, AP1S1, SERINC3, CCK, PLK2, NCALD and ICAM5
GSE132903 and GSE5281	ERICH3, TUBB2A, NSF and GLRB
GSE122063 and GSE5281	PAX7, GDA, MET, SERPINF1, LINC00460, SYT13, LOC283484, TASP1, TSPAN7, ACOT7, SARS, CHRM1, CHRNB2, GPATCH2, KRT222, NMNAT2, UBE2N, ZCCHC12, GPR158, SDR16C5, ENO2, FGF12, CD200, FPGT-TNNI3K, RBM3, GAP43, ERC2, GNG2, RNF175, PPM1E, TARBP1, UBE2QL1, SYN2, ATL1, AMPH, SLC1A6, GNG3, NECAP1, MYT1L, NAP1L5, TAGLN3, C14orf79, GABRD, UNC13A, GLS, SOSTDC1, NRXN3, LY86-AS1, ATP8A2, SH3GL2, MLLT11, STMN2, BRWD1, MAP4, PPM1J, RAB3C, UCHL1, WDR54, MDH1, BDNF, DCLK1, STAT4, VSNL1, GPRASP2, EPHA5, PNMAL2, CITED1, NUDT18, TRIM37, FAR2, PCLO, SV2B, RAB27B, SNAP25, GOLGA8A, HMP19, SVOP, LOC100506124, PAK3, CDC42, SYCE1, CAMK1G, CCKBR, TUBB3, COPG2IT1, PPP1R2, RBP4, PPEF1, NOP56, INA, CACNG3, MICAL2, PTPRO, LOC100129973, BSCL2, PTPN3, CIRBP, PLD3, HS6ST3, PPP1R14C, ATOH7, SCG5, MAL2, NPTXR, BEX5 and GLS2
GSE132903 and GSE15222	SERPINI1
GSE132903 and GSE15222	SCG2, VIP, KCNV1, GRP, NMU, HSPB3, TMEM155 and PCDH8
GSE122063 and GSE48350	SLC32A1
GSE122063 and GSE132903	CAP2

PPI analysis:

Around 18 LDGs were selected from NCBI portal (Table-4) and were subjected to PPI analysis with the shortlisted DEGs from the above step. PPI analysis (Fig. 5) revealed that BDNF exhibited highest node degree (16) followed by SST (7), AACT (SERPINA3) (4), RTN3 (2), RGS4 (3), NPTX (1) and CRYM (1). BDNF exhibited high connectivity with

AD specific proteins like Glutamate Ionotropic Receptor NMDA Type Subunit 2B (GRIN2B), BACE1, MAPT, PSEN1, TP53, BCHE, SNCA, COMT, INS, APP, APOE and ACHE. SST exhibited PPI with IDE, MME, IGF, APP, INS and ACHE. SERPINA3/AACT exhibited interactions with APOA1, APOE and APP proteins. RTN3 interacted with BACE1 and APP. RGS4 interacted with COMT alone. NPTX and CRYM did not exhibit interactions with any of LDGs (Fig. 5, Table-5 & 6).

Table-4 List of LDGs retrieved from NCBI

Gene symbol	NCBI gene ID	HUGO Gene Nomenclature Committee (HGCN) ID	Chromosome location	Reference
APOE	348	HGNC:613	19q13.32	[48]
APP	351	HGNC:620	21q21.3	[49]
GRIN2B	2904	HGNC:4586	12p13.1	[50]
SNCA	6622	HGNC:11138	4q22.1	[51]
MAPT	4137	HGNC:6893	17q21.31	[52]
COMT	1312	HGNC:2228	22q11.21	[53]
TP53	7157	HGNC:11998	17p13.1	[54]
AGER	177	HGNC:320	6p21.32	[55]
IGF1	3479	HGNC:5464	12q23.2	[56]
PSEN1	5663	HGNC:9508	14q24.2	[52]
BACE1	23621	HGNC:933	11q23.3	[57]
INS	3630	HGNC:6081	11p15.5	[56]
APOA1	335	HGNC:600	11q23.3	[58]
LDLR	3949	HGNC:6547	19p13.2	[59]
ACHE	43	HGNC:108	7q22.1	[60]
BCHE	590	HGNC:983	3q26.1	[60]
IDE	3416	HGNC:5381	10q23.33	[61]
NEP	4311	HGNC:7154	3q25.2	[61]

Table-5 Significant PPI of identified DEGs with LDGs

Node 1	Node 2	Combined Score
BDNF	TP53	0.95
	IGF1	0.894
	APP	0.828
	APOE	0.81
	PSEN1	0.781
	COMT	0.733
	INS	0.715
	SNCA	0.708
	ACHE	0.657
	MAPT	0.598
	BACE1	0.594
	BCHE	0.518
	GRIN2B	0.982
SST	APP	0.928
	INS	0.915
	IGF1	0.791
	IDE	0.59
	ACHE	0.579
	MME/NEP	0.404
AACT/SERPINA3	APP	0.476
	APOA1	0.45
	APOE	0.609
RTN3	APP	0.523
	BACE1	0.8
RGS4	COMT	0.641

Table -6 Characteristics of PPI network

Node Name	Average Shortest Path Length	Betweenness Centrality	Clustering Coefficient	Node Degree	Neighborhood Connectivity	Radiality	Topological Coefficient
APP	1.214286	0.167659	0.399209	23	10.26087	0.946429	0.380032
APOE	1.214286	0.171997	0.403162	23	10.3913	0.946429	0.384863
PSEN1	1.392857	0.045109	0.555556	18	12.05556	0.901786	0.446502
INS	1.392857	0.055697	0.542484	18	12	0.901786	0.444444
BACE1	1.428571	0.052044	0.573529	17	12.29412	0.892857	0.455338
BDNF	1.428571	0.1859	0.525	16	11.875	0.892857	0.4375
MAPT	1.535714	0.014431	0.703297	14	13.71429	0.866071	0.507937
SNCA	1.642857	0.00439	0.836364	11	15.27273	0.839286	0.565657
TP53	1.642857	0.011054	0.763636	11	14.90909	0.839286	0.552189
ACHE	1.642857	0.009583	0.745455	11	15.09091	0.839286	0.558923
IGF1	1.678571	0.003503	0.844444	10	15.8	0.830357	0.585185
BCHE	1.714286	0.002774	0.861111	9	16.44444	0.821429	0.609054
IDE	1.75	0.004939	0.781818	11	14.36364	0.8125	0.574545
COMT	1.75	0.035647	0.464286	8	10.375	0.8125	0.384259
SST	1.785714	0.003489	0.761905	7	14.14286	0.803571	0.52381
MME	1.785714	0.007593	0.711111	10	14	0.803571	0.56
GRIN2B	1.821429	0.001563	0.8	6	17	0.794643	0.62963
LDLR	1.892857	0.001436	0.857143	7	16.28571	0.776786	0.651429
APOA1	1.892857	0.005669	0.666667	7	12.42857	0.776786	0.497143
AGER	1.892857	0	1	7	17.14286	0.776786	0.685714
AACT	2	0	1	4	14.25	0.75	0.57
GIG25	2	0	1	4	14.25	0.75	0.57
RTN3	2.142857	0	1	2	20	0.714286	0.869565
RGS4	2.25	0.071429	0.333333	3	8.333333	0.6875	0.470588
NPTX2	2.392857	0	0	1	16	0.651786	0
CRYM	3.214286	0	0	1	3	0.446429	0

Functional Enrichment Analysis:

The common DEGs retrieved were subjected to functional enrichment analysis to explore their involvement in Gene Ontology (GO) and Kyoto Encyclopedia of Genes and Genomes (KEGG) pathways.

GO analysis revealed that SLC5A3 was involved in transport of potassium ions across plasma membrane (GO:0098739) and peripheral nervous system development (GO:0007422), whereas BDNF, RGS4, NPTX2 and SST were involved in cognitive abilities (GO:0050890), trans-synaptic signalling (GO:0099157), striated muscle cell differentiation (GO:0051154), anterograde trans-synaptic transmission (GO:0098916) and regulation of nervous system process (GO:0031644). BDNF, SST and ENC1 were involved in receptor ligand activity (GO:0048018), cytokine receptor binding (GO:0005126), positive regulation of cell projection organization (GO:0031346) and receptor regulator activity (GO:0030545). ENC1 and RTN3 were found to be involved in negative regulation of cellular amide metabolic process (GO:0034249). SERPINA3 in combination with SST was known to be involved in digestion (GO:0007586) (Fig. 6).

KEGG analysis revealed that BDNF was involved in triggering Phospholnositide 3-Kinase (PI3K) pathway (hsa04213), Rat Sarcoma (RAS) signalling (hsa05212), RAC1 signalling (hsa04510), FYN signalling (hsa04380), CDK5 (Cyclin Dependent Kinase 5) phosphorylation, FYN mediated GRIN2B activation and transcriptional signalling. BDNF and SST were involved in transcription regulation by Methyl-CpG Binding Protein 2 (MECP2), gastric acid secretion (hsa04971) and somatostatin gene expression. RGS4 was known to mediate G alpha (i) auto-inactivation and G alpha (q) inactivation by hydrolysing Guanine Tri Phosphate (GTP) to Guanine Di Phosphate (GDP). CRYM was involved in Lysine catabolism, autosomal dominant deafness, whereas, RTN3 was involved in protein-protein interactions at synapses, binding of Synaptic Adhesion-Like Molecule 1-4 (SALM1-4) to reticulons and synaptic adhesion like molecules. SERPINA3 was involved in exocytosis of platelet alpha granules and azurophil granule lumen proteins (Fig. 7).

Discussion

This study aimed to retrieve significant DEGs associated with AD by analysing the gene expression data available in GEO database. Initially, the GEO datasets were selected based on the inclusion and exclusion criteria which resulted in 32 datasets. The raw data for each dataset was analysed individually through Bioconductor package in R and DEGs with FDR p-value <0.05 were retrieved and segregated into upregulated and downregulated DEGs. Though 32 datasets were found to be eligible, only 16 datasets satisfied the initial criteria FDR p-value < 0.05. These DEGs were subjected to screening based on different filtering norms and this yielded 6 datasets with both upregulated and downregulated DEGs and overlapping DEGs were found in 60% of these datasets. SLC5A3 and SERPINA3 were found to be common in upregulated DEGs whereas, SST, BDNF, RGS4, CRYM, NPTX2, RTN3 and ENC1 were found to be common in downregulated DEGs. These DEGs were further subjected to PPI analysis with 18 LDGs which were known to possess a strong role in AD pathogenesis. Among the above 9 DEGs, BDNF, SST, SERPINA3(AACT), RTN3 and RGS4 exhibited significant interactions.

BDNF exhibited interaction with most crucial targets like GRIN2B, BACE1, APP, MAPT, SNCA, ACHE, APOE, PSEN1, COMT etc. Functional enrichment analysis revealed the normal physiological role of BDNF in cytokine signalling, receptor ligand activity and its regulation, trans-synaptic signalling, cognitive functions, chemical synaptic transmission, cell differentiation, cell growth and its regulation. This suggests its crucial involvement in neuronal growth, development and transmission which was found to be abnormal in AD. KEGG pathway analysis revealed detailed mechanistic action of BDNF. BDNF initiates its response by binding to Tyrosine Kinase Beta (TRKβ) receptor, post binding the receptor dimerizes and undergoes autophosphorylation. The phosphorylated TRKβ triggers various signalling mechanisms such PI3K, RAS, CDK5, RAC1 GTPase, Src Homology 2 Domain-Containing 1 (SHC1), FYN kinase, Fibroblast Growth Factor Receptor Substrate 2 (FRS2), T-Lymphoma Invasion And Metastasis-Inducing Protein 1 (TIAM1), Phospholipase C Gamma 1 (PLCG1) etc., These were in turn found to be involved in triggering secondary signalling pathways through GRIN2B which is associated with cocaine addiction, cognitive central hypoventilation syndrome and eating disorders. A number of research studies have reported downregulation of BDNF expression which is online with our findings [62][63].

The PPI analysis of SST portrayed its interaction with primary AD targets like IDE, MME, IGF, APP, INS and ACHE. Alike BDNF, SST also exhibited its physiological role in trans-synaptic signalling, cognitive activities, anterograde trans-synaptic signalling, receptor ligand activity, cytokine receptor binding and receptor regulator activity. KEGG pathway analysis revealed the association of SST with MECP2 and c-AMP Responsive Element Binding protein 1 (CREB1). It is reported that MECP2 together with CREB1 enhances the expression of SST by binding to the

promoter region [64]. There are five subtypes of SST receptors, out of which, three receptors viz., SSTR2, SSTR4 and SSTR5 were observed to display a marked downregulation and reduced sensitivity in AD. This interferes with their inhibitory control over Adenyl Cyclase (AC) pathway. Decreased SSTR2 results in decreased Neprilysin activity, an enzyme involved in degradation of Aβ peptides [65][66][67]. In addition, post-mortem AD brains with reduced SST receptors were corelated with higher degree of amnesia and cognitive dysfunction [68][69]. In concordance with the above studies, our analysis found downregulation of SST receptors.

SERPINA3 or AACT is a 55-68 kDa serine protease inhibitor secreted by epididymal cells of choroid plexus [70]. Our PPI analysis identified its interaction with APP, APOE and APOA1. Functional enrichment analysis revealed its role in digestion and exocytosis. In AD, it was reported to be colocalized with amyloid plaques. The hydrophobic domain at C-terminal of this enzyme interacts and forms complex with amyloid fibrils. These complexes are known to upregulate SERPINA3 resulting in disruption of cognitive functions [71][72]. Apart from interacting with Aβ fibrils, it was also known to promote tau phosphorylation at Ser202, Thr231, Ser396 and Thr404 by augmenting Extracellular signal Related Kinase (ERK), Glycogen Synthase Kinase-3β (GSK-3) and c-Jun N-terminal Kinase (JNK) leading to inflammatory responses promoting neuronal death and degeneration [73][74].

RTN3, a transmembrane Endoplasmic Reticulum (ER) protein, belongs to a family of Reticulons. Reticulons consists of four mammalian paralogues viz., RTN1, RTN2, RTN3 and RTN4, out of which, RTN3 and RTN4 are neuronal specific. The members of this reticulon family possess conserved QID triplet region called as Reticulon Homology Domain (RHD) in their C-terminal region. This RHD domain was found to interact with C-terminal domain of BACE1, which is involved in formation of Aβ peptides [75][76][77]. The BACE1-RTN3 complex is reported to halt the axonal transport and enzymatic activity of BACE1 on APP, thereby terminating the amyloidogenic pathway. It was also reported that BACE1 was found to specifically interact with monomeric RTN3 rather than dimeric forms [78][76]. The formation of RTN3 aggregates was found to be regulated by B-cell Receptor Associated Protein 31 (BAP31), an integral ER membrane protein. Silencing of this gene leads to formation of RTN3 aggregates, thereby reducing the interaction with BACE1 which promotes Aβ formation [79][80]. Our functional enrichment analysis revealed the interactions of RTN3 with synaptic proteins and gene expression analysis demonstrated downregulation of this gene.

RGS4, a member of family RGS modulates the G-protein signalling activity by inhibiting AC and Phospho Lipase C (PLC) activity. RGS4 inhibits GPCR mediated APP cleavage, while downregulation of RGS4 enhances APP cleavage [81]. Functional enrichment analysis revealed that RGS4 was involved in various regulatory activities like modulation of chemical synaptic transmission, regulation of trans-synaptic signalling, nervous process, striated muscle cell differentiation, regulation of cell growth etc., KEGG analysis revealed that active G alpha (i), (q) and (z) as binding partners of RGS4. Our gene expression analysis revealed downregulation of RGS4 in AD cases.

In a nutshell, from the analysis, BDNF, SST, SERPINA3, RTN3 and RGS4 were found to be crucially involved in AD pathogenesis. BDNF and SST trigger various signalling mechanisms like PKA, PI3K and AKT, which in turn inhibit the GSK3β and BAD activity. This process results in inhibition of apoptosis and promotion of neuronal growth. On the other hand, downregulation of BDNF and SST enables Aβ fibrils to inhibit the aforementioned signalling mechanisms, thereby resulting in enhanced apoptosis and neuronal cell death. RTN3 interacts with BACE1 directly and inhibits its accession to APP cleavage, thereby promoting the non-amyloidogenic pathway. RGS4 acts in similar fashion as SST by hindering GTP hydrolysis (Fig. 8). Presence of Aβ fibrils lead to AD progression, however, the aforesaid targets are believed to have substantial potential to counteract Aβ toxicity.

Conclusion

Systematic analysis of the metadata by considering all the AD related genetic datasets with a developed set of filtering criteria improved the precision of the results. Through this analysis, SLC5A3, BDNF, SST, SERPINA3, RTN3, RGS4, NPTX, ENC1 and CRYM were identified as potential genes involved in AD pathogenesis. Among the identified genes, BDNF, SST, SERPINA3, RTN3 and RGS4 exhibited significant interactions with LDGs and thus they were considered to play a major role in AD progression.

List Of Abbreviations

Acronym	Abbrevation
Aβ	Amyloid Beta plaques
AC	Adenyl Cyclase
AD	Alzheimer’s Disease
APP	Amyloid Precursor Protein
ARDSI	Alzheimer’s and Related Disorders Society of India
BACE-1	Beta-Secretase 1
BAP31	B-cell Receptor Associated Protein 31
BDNF	Brain Derived Neurotrophic Factor
CDK5	Cyclin Dependent Kinase 5
COVID-19	Corona Virus Disease 19
CREB1	c-AMP Responsive Element Binding protein 1
CRYM	Crystallin Mu
DEGs	Differentially Expressed Genes
ENC1	Ectodermal-Neural Cortex 1
ERK	Extracellular signal Related Kinase
FC	Fold Change
FDR	False Discovery Rate
FRS2	Fibroblast Growth Factor Receptor Substrate 2
GEO	Gene Expression Omnibus
GDP	Guanine Di Phosphate
GTP	Guanine Tri Phosphate
GRIN2B	Glutamate Ionotropic Receptor NMDA Type Subunit 2B
GSK-3β	Glycogen Synthase Kinase-3β
HGCN	HUGO Gene Nomenclature Committee
JNK	c-Jun N-terminal Kinase
LDGs	Literature Derived Genes
MAPT	Microtubule Associated Protein Tau
MECP2	Methyl-CpG Binding Protein 2
NCBI	National Centre for Biotechnology Information
NFT	Neurofibrillary Tangles
NPTX2	Neuronal Pentraxin 2
PI3K	PhosphoInositide 3-Kinase
PLC	Phospho Lipase C
PLCG1	Phospholipase C Gamma 1
PPI	Protein-Protein Interaction
PSEN1	Presenilin 1
RAS	Rat Sarcoma
RGS4	Regulator of G Protein Signalling 4
RHD	Reticulon Homology Domain
SALM1-4	Synaptic Adhesion-Like Molecule 1-4
SERPINA3	Serpin Family A Member 3
SHC1	Src Homology 2 Domain-Containing 1
SLC5A3	Solute Carrier Family 5 Member 3
SST	Somatostatin

STRING	Search Tool for the Retrieval of Interacting Genes/Proteins
TIAM1	T-Lymphoma Invasion And Metastasis-Inducing Protein 1
TRKβ	Tyrosine Kinase Beta
US-FDA	U.S. Food and Drug Administration

Declarations

Ethics approval and consent to participate: NA

Consent for publication: NA

Availability of data and materials:

The datasets generated and/or analysed during the current study are available in the GEO database

1. https://www.ncbi.nlm.nih.gov/geo/query/acc.cgi?acc=GSE36980
2. https://www.ncbi.nlm.nih.gov/geo/query/acc.cgi?acc=GSE28146
3. https://www.ncbi.nlm.nih.gov/geo/query/acc.cgi?acc=GSE4757
4. https://www.ncbi.nlm.nih.gov/geo/query/acc.cgi?acc= GSE4226
5. https://www.ncbi.nlm.nih.gov/geo/query/acc.cgi?acc= GSE1279
6. https://www.ncbi.nlm.nih.gov/geo/query/acc.cgi?acc= GSE110226
7. https://www.ncbi.nlm.nih.gov/geo/query/acc.cgi?acc= GSE93885
8. https://www.ncbi.nlm.nih.gov/geo/query/acc.cgi?acc= GSE97760
9. https://www.ncbi.nlm.nih.gov/geo/query/acc.cgi?acc= GSE63060
10. https://www.ncbi.nlm.nih.gov/geo/query/acc.cgi?acc= GSE63061
11. https://www.ncbi.nlm.nih.gov/geo/query/acc.cgi?acc= GSE5281
12. https://www.ncbi.nlm.nih.gov/geo/query/acc.cgi?acc= GSE6384
13. https://www.ncbi.nlm.nih.gov/geo/query/acc.cgi?acc= GSE12685
14. https://www.ncbi.nlm.nih.gov/geo/query/acc.cgi?acc= GSE4227
15. https://www.ncbi.nlm.nih.gov/geo/query/acc.cgi?acc= GSE4229
16. https://www.ncbi.nlm.nih.gov/geo/query/acc.cgi?acc= GSE15222
17. https://www.ncbi.nlm.nih.gov/geo/query/acc.cgi?acc= GSE18309
18. https://www.ncbi.nlm.nih.gov/geo/query/acc.cgi?acc= GSE16759
19. https://www.ncbi.nlm.nih.gov/geo/query/acc.cgi?acc= GSE32645
20. https://www.ncbi.nlm.nih.gov/geo/query/acc.cgi?acc= GSE26927
21. https://www.ncbi.nlm.nih.gov/geo/query/acc.cgi?acc= GSE61196
22. https://www.ncbi.nlm.nih.gov/geo/query/acc.cgi?acc= GSE33000
23. https://www.ncbi.nlm.nih.gov/geo/query/acc.cgi?acc= GSE37264
24. https://www.ncbi.nlm.nih.gov/geo/query/acc.cgi?acc= GSE48350
25. https://www.ncbi.nlm.nih.gov/geo/query/acc.cgi?acc= GSE132903

26. https://www.ncbi.nlm.nih.gov/geo/query/acc.cgi?acc= GSE131617
27. https://www.ncbi.nlm.nih.gov/geo/query/acc.cgi?acc= GSE122063
28. https://www.ncbi.nlm.nih.gov/geo/query/acc.cgi?acc= GSE26972
29. https://www.ncbi.nlm.nih.gov/geo/query/acc.cgi?acc= GSE37263
30. https://www.ncbi.nlm.nih.gov/geo/query/acc.cgi?acc= GSE118553
31. https://www.ncbi.nlm.nih.gov/geo/query/acc.cgi?acc=GSE13214
32. https://www.ncbi.nlm.nih.gov/geo/query/acc.cgi?acc=GSE29378

Competing interests: The authors declare that they have no competing interests

Funding: NA

Authors' contributions

GNS analyzed the data and drafted the manuscript. GRS and R Burri supervised the work and finalized the manuscript.

Acknowledgements: We thank Pharmacological Modelling and Simulation Centre (PMSC) research centre and members of M.S. Ramaiah University of Applied Sciences, Bangalore for their support throughout the work.

Author Details:

Hema Sree G N S: Research Scholar, Pharmacological Modelling and Simulation Centre, Faculty of Pharmacy, M. S. Ramaiah University of Applied Sciences, Bangalore, India

Orcid ID: https://orcid.org/0000-0001-7165-5272

Email ID: nagasai.hemasree615@gmail.com

Saraswathy Ganesan Rajalekshmi: Associate Professor, Deparment of Pharmacy Practice, Faculty of Pharmacy, Head, Pharmacological Modelling and Simulation Centre, M. S. Ramaiah University of Applied Sciences, Bangalore, India

Orcid ID: 0000-0001-7279-3765

Email ID: saraswathypradish@gmail.com

Raghunadha R Burri: Associate director, IT BPE, Dr. Reddy's Laboratories Limited, Hyderabad, Telangana 500034

Email ID: rburri@gmail.com

References

1. International D. World Alzheimer Report 2018 - The state of the art of dementia research: New frontiers; World Alzheimer Report 2018 - The state of the art of dementia research: New frontiers. https://www.alz.co.uk/research/WorldAlzheimerReport2018.pdf. Accessed 10 May 2019.
2. Alzheimer’s disease facts and figures. Alzheimer’s Dement. 2021;17:327–406. doi:10.1002/alz.12328.

3. Kumar CTS, Shaji KS, Varghese M NM (Eds). DEMENTIA IN INDIA 2020 2. Alzheimer's and Related Disorders Society of India (ARDSI), Cochin; 2020.
4. Chouraki V, Seshadri S. Genetics of Alzheimer's disease. Elsevier; 2014. doi:10.1016/B978-0-12-800149-3.00005-6.
5. Barrett T, Wilhite SE, Ledoux P, Evangelista C, Kim IF, Tomashevsky M, et al. NCBI GEO: archive for functional genomics data sets–update. Nucleic Acids Res. 2013;41 Database issue:D991-5. doi:10.1093/nar/gks1193.
6. Brown GR, Hem V, Katz KS, Ovetsky M, Wallin C, Ermolaeva O, et al. Gene: a gene-centered information resource at NCBI. Nucleic Acids Res. 2015;43:D36–42. doi:10.1093/nar/gku1055.
7. von Mering C, Huynen M, Jaeggi D, Schmidt S, Bork P, Snel B. STRING: a database of predicted functional associations between proteins. Nucleic Acids Res. 2003;31:258–61. http://www.ncbi.nlm.nih.gov/pubmed/12519996. Accessed 24 Jul 2018.
8. Bindea G, Mlecnik B, Hackl H, Charoentong P, Tosolini M, Kirilovsky A, et al. ClueGO: a Cytoscape plug-in to decipher functionally grouped gene ontology and pathway annotation networks. Bioinformatics. 2009;25:1091–3. doi:10.1093/bioinformatics/btp101.
9. Hokama M, Oka S, Leon J, Ninomiya T, Honda H, Sasaki K, et al. Altered expression of diabetes-related genes in Alzheimer's disease brains: The Hisayama study. Cereb Cortex. 2014;24:2476–88.
10. Blalock EM, Buechel HM, Popovic J, Geddes JW, Landfield PW. Microarray analyses of laser-captured hippocampus reveal distinct gray and white matter signatures associated with incipient Alzheimer's disease. J Chem Neuroanat. 2011;42:118–26. doi:10.1016/j.jchemneu.2011.06.007.
11. Dunckley T, Beach TG, Ramsey KE, Grover A, Mastroeni D, Walker DG, et al. Gene expression correlates of neurofibrillary tangles in Alzheimer's disease. Neurobiol Aging. 2006;27:1359–71. doi:10.1016/j.neurobiolaging.2005.08.013.
12. Maes OC, Xu S, Yu B, Chertkow HM, Wang E, Schipper HM. Transcriptional profiling of Alzheimer blood mononuclear cells by microarray. Neurobiol Aging. 2007;28:1795–809. doi:10.1016/j.neurobiolaging.2006.08.004.
13. Maes OC, Schipper HM, Chertkow HM, Wang E. Methodology for discovery of Alzheimer's disease blood-based biomarkers. Journals Gerontol - Ser A Biol Sci Med Sci. 2009;64:636–45. doi:10.1093/gerona/glp045.
14. Blalock EM, Geddes JW, Chen KC, Porter NM, Markesbery WR, Landfield PW. Incipient Alzheimer's disease: Microarray correlation analyses reveal major transcriptional and tumor suppressor responses. Proc Natl Acad Sci U S A. 2004;101:2173–8. doi:10.1073/pnas.0308512100.
15. Stopa EG, Tanis KQ, Miller MC, Nikonova E V., Podtelezhnikov AA, Finney EM, et al. Comparative transcriptomics of choroid plexus in Alzheimer's disease, frontotemporal dementia and Huntington's disease: Implications for CSF homeostasis. Fluids Barriers CNS. 2018;15. doi:10.1186/s12987-018-0102-9.
16. Kant S, Stopa EG, Johanson CE, Baird A, Silverberg GD. Choroid plexus genes for CSF production and brain homeostasis are altered in Alzheimer's disease. Fluids Barriers CNS. 2018;15. doi:10.1186/s12987-018-0120-7.
17. Lachen-Montes M, Zelaya MV, Segura V, Fernández-Irigoyen J, Santamaría E. Progressive modulation of the human olfactory bulb transcriptome during Alzheimer's disease evolution: Novel insights into the olfactory signaling across proteinopathies. Oncotarget. 2017;8:69663–79. doi:10.18632/oncotarget.18193.
18. Naughton BJ, Duncan FJ, Murrey DA, Meadows AS, Newsom DE, Stoicea N, et al. Blood genome-wide transcriptional profiles reflect broad molecular impairments and strong blood-brain links in Alzheimer's

disease. J Alzheimer's Dis. 2014;43:93–108. doi:10.3233/JAD-140606.

19. Sood S, Gallagher IJ, Lunnon K, Rullman E, Keohane A, Crossland H, et al. A novel multi-tissue RNA diagnostic of healthy ageing relates to cognitive health status. Genome Biol. 2015;16. doi:10.1186/s13059-015-0750-x.
20. Liang WS, Dunckley T, Beach TG, Grover A, Mastroeni D, Walker DG, et al. Gene expression profiles in anatomically and functionally distinct regions of the normal aged human brain. Physiol Genomics. 2007;28:311–22. doi:10.1152/physiolgenomics.00208.2006.
21. Liang WS, Reiman EM, Valla J, Dunckley T, Beach TG, Grover A, et al. Alzheimer's disease is associated with reduced expression of energy metabolism genes in posterior cingulate neurons. Proc Natl Acad Sci U S A. 2008;105:4441–6. doi:10.1073/pnas.0709259105.
22. Readhead B, Haure-Mirande JV, Funk CC, Richards MA, Shannon P, Haroutunian V, et al. Multiscale Analysis of Independent Alzheimer's Cohorts Finds Disruption of Molecular, Genetic, and Clinical Networks by Human Herpesvirus. Neuron. 2018;99:64-82.e7. doi:10.1016/j.neuron.2018.05.023.
23. Liang WS, Dunckley T, Beach TG, Grover A, Mastroeni D, Ramsey K, et al. Altered neuronal gene expression in brain regions differentially affected by Alzheimer's disease: A reference data set. Physiol Genomics. 2008;33:240–56. doi:10.1152/physiolgenomics.00242.2007.
24. Heinzen EL, Yoon W, Weale ME, Sen A, Wood NW, Burke JR, et al. Alternative ion channel splicing in mesial temporal lobe epilepsy and Alzheimer's disease. Genome Biol. 2007;8. doi:10.1186/gb-2007-8-3-r32.
25. Williams C, Shai RM, Wu Y, Hsu YH, Sitzer T, Spann B, et al. Transcriptome analysis of synaptoneurosomes identifies neuroplasticity genes overexpressed in incipient Alzheimer's disease. PLoS One. 2009;4. doi:10.1371/journal.pone.0004936.
26. Maes OC, Schipper HM, Chong G, Chertkow HM, Wang E. A GSTM3 polymorphism associated with an etiopathogenetic mechanism in Alzheimer disease. Neurobiol Aging. 2010;31:34–45. doi:10.1016/j.neurobiolaging.2008.03.007.
27. Webster JA, Gibbs JR, Clarke J, Ray M, Zhang W, Holmans P, et al. Genetic Control of Human Brain Transcript Expression in Alzheimer Disease. Am J Hum Genet. 2009;84:445–58. doi:10.1016/j.ajhg.2009.03.011.
28. Chen K Den, Chang PT, Ping YH, Lee HC, Yeh CW, Wang PN. Gene expression profiling of peripheral blood leukocytes identifies and validates ABCB1 as a novel biomarker for Alzheimer's disease. Neurobiol Dis. 2011;43:698–705. doi:10.1016/j.nbd.2011.05.023.
29. Nunez-Iglesias J, Liu CC, Morgan TE, Finch CE, Zhou XJ. Joint genome-wide profiling of miRNA and mRNA expression in Alzheimer's disease cortex reveals altered miRNA regulation. PLoS One. 2010;5. doi:10.1371/journal.pone.0008898.
30. Fischer MT, Wimmer I, Höftberger R, Gerlach S, Haider L, Zrzavy T, et al. Disease-specific molecular events in cortical multiple sclerosis lesions. Brain. 2013;136:1799–815. doi:10.1093/brain/awt110.
31. Durrenberger PF, Fernando FS, Magliozzi R, Kashefi SN, Bonnert TP, Ferrer I, et al. Selection of novel reference genes for use in the human central nervous system: A BrainNet Europe Study. Acta Neuropathol. 2012;124:893–903. doi:10.1007/s00401-012-1027-z.
32. Durrenberger PF, Fernando FS, Kashefi SN, Bonnert TP, Seilhean D, Nait-Oumesmar B, et al. Common mechanisms in neurodegeneration and neuroinflammation: a BrainNet Europe gene expression microarray study. J Neural Transm. 2015;122:1055–68. doi:10.1007/s00702-014-1293-0.
33. Bergen AA, Kaing S, ten Brink JB, Gorgels TG, Janssen SF. Gene expression and functional annotation of human choroid plexus epithelium failure in Alzheimer's disease. BMC Genomics. 2015;16.

doi:10.1186/s12864-015-2159-z.

34. Narayanan M, Huynh JL, Wang K, Yang X, Yoo S, McElwee J, et al. Common dysregulation network in the human prefrontal cortex underlies two neurodegenerative diseases. Mol Syst Biol. 2014;10:743. doi:10.15252/msb.20145304.
35. Lai MKP, Esiri MM, Tan MGK. Genome-wide profiling of alternative splicing in Alzheimer's disease. Genomics Data. 2014;2:290–2. doi:10.1016/j.gdata.2014.09.002.
36. Berchtold NC, Coleman PD, Cribbs DH, Rogers J, Gillen DL, Cotman CW. Synaptic genes are extensively downregulated across multiple brain regions in normal human aging and Alzheimer's disease. Neurobiol Aging. 2013;34:1653–61. doi:10.1016/j.neurobiolaging.2012.11.024.
37. Cribbs DH, Berchtold NC, Perreau V, Coleman PD, Rogers J, Tenner AJ, et al. Extensive innate immune gene activation accompanies brain aging, increasing vulnerability to cognitive decline and neurodegeneration: A microarray study. J Neuroinflammation. 2012;9. doi:10.1186/1742-2094-9-179.
38. Astarita G, Jung KM, Berchtold NC, Nguyen VQ, Gillen DL, Head E, et al. Deficient liver biosynthesis of docosahexaenoic acid correlates with cognitive impairment in Alzheimer's disease. PLoS One. 2010;5:1–8. doi:10.1371/journal.pone.0012538.
39. Blair LJ, Nordhues BA, Hill SE, Scaglione KM, O'Leary JC, Fontaine SN, et al. Accelerated neurodegeneration through chaperone-mediated oligomerization of tau. J Clin Invest. 2013;123:4158–69. doi:10.1172/JCI69003.
40. Piras IS, Krate J, Delvaux E, Nolz J, Mastroeni DF, Persico AM, et al. Transcriptome Changes in the Alzheimer's Disease Middle Temporal Gyrus: Importance of RNA Metabolism and Mitochondria-Associated Membrane Genes. J Alzheimer's Dis. 2019;70:691–713. doi:10.3233/JAD-181113.
41. Miyashita A, Hatsuta H, Kikuchi M, Nakaya A, Saito Y, Tsukie T, et al. Genes associated with the progression of neurofibrillary tangles in alzheimer's disease. Transl Psychiatry. 2014;4. doi:10.1038/tp.2014.35.
42. McKay EC, Beck JS, Khoo SK, Dykema KJ, Cottingham SL, Winn ME, et al. Peri-infarct upregulation of the oxytocin receptor in vascular dementia. J Neuropathol Exp Neurol. 2019;78:436–52. doi:10.1093/jnen/nlz023.
43. Berson A, Barbash S, Shaltiel G, Goll Y, Hanin G, Greenberg DS, et al. Cholinergic-associated loss of hnRNP-A/B in Alzheimer's disease impairs cortical splicing and cognitive function in mice. EMBO Mol Med. 2012;4:730–42. doi:10.1002/emmm.201100995.
44. Tan MG, Chua WT, Esiri MM, Smith AD, Vinters H V., Lai MK. Genome wide profiling of altered gene expression in the neocortex of Alzheimer's disease. J Neurosci Res. 2010;88:1157–69. doi:10.1002/jnr.22290.
45. Patel H, Hodges AK, Curtis C, Lee SH, Troakes C, Dobson RJB, et al. Transcriptomic analysis of probable asymptomatic and symptomatic alzheimer brains. Brain Behav Immun. 2019;80:644–56. doi:10.1016/j.bbi.2019.05.009.
46. Miller JA, Woltjer RL, Goodenbour JM, Horvath S, Geschwind DH. Genes and pathways underlying regional and cell type changes in Alzheimer's disease. Genome Med. 2013;5. doi:10.1186/gm452.
47. Silva ART, Grinberg LT, Farfel JM, Diniz BS, Lima LA, Silva PJS, et al. Transcriptional Alterations Related to Neuropathology and Clinical Manifestation of Alzheimer's Disease. PLoS One. 2012;7. doi:10.1371/journal.pone.0048751.
48. Nho K, Kim S, Horgusluoglu E, Risacher SL, Shen L, Kim D, et al. Association analysis of rare variants near the APOE region with CSF and neuroimaging biomarkers of Alzheimer's disease. BMC Med Genomics. 2017;10:29. doi:10.1186/s12920-017-0267-0.

49. Schrötter A, Pfeiffer K, El Magraoui F, Platta HW, Erdmann R, Meyer HE, et al. The amyloid precursor protein (APP) family members are key players in S-adenosylmethionine formation by MAT2A and modify BACE1 and PSEN1 gene expression-relevance for Alzheimer's disease. Mol Cell Proteomics. 2012;11:1274–88. doi:10.1074/mcp.M112.019364.
50. Andreoli V, De Marco EV, Trecroci F, Cittadella R, Di Palma G, Gambardella A. Potential involvement of GRIN2B encoding the NMDA receptor subunit NR2B in the spectrum of Alzheimer's disease. J Neural Transm. 2013;121:533–42. doi:10.1007/s00702-013-1125-7.
51. Mackin RS, Insel P, Zhang J, Mohlenhoff B, Galasko D, Weiner M, et al. Cerebrospinal fluid α-synuclein and Lewy body-like symptoms in normal controls, mild cognitive impairment, and Alzheimer's disease. J Alzheimers Dis. 2015;43:1007–16. doi:10.3233/JAD-141287.
52. Sassi C, Guerreiro R, Gibbs R, Ding J, Lupton MK, Troakes C, et al. Investigating the role of rare coding variability in Mendelian dementia genes (APP, PSEN1, PSEN2, GRN, MAPT, and PRNP) in late-onset Alzheimer's disease. Neurobiol Aging. 2014;35:2881.e1-2881.e6. doi:10.1016/j.neurobiolaging.2014.06.002.
53. Zhou J, Li X-M, Jiang T, Liu Y, Chi S, Yu J-T, et al. Lack of association between COMT Val158Met polymorphism and late-onset Alzheimer's disease in Han Chinese. Neurosci Lett. 2013;554:162–6. doi:10.1016/J.NEULET.2013.09.006.
54. Wojsiat J, Laskowska-Kaszub K, Alquézar C, Białopiotrowicz E, Esteras N, Zdioruk M, et al. Familial Alzheimer's Disease Lymphocytes Respond Differently Than Sporadic Cells to Oxidative Stress: Upregulated p53-p21 Signaling Linked with Presenilin 1 Mutants. Mol Neurobiol. 2017;54:5683–98. doi:10.1007/s12035-016-0105-y.
55. Deane R, Yan S Du, Submamaryan RK, LaRue B, Jovanovic S, Hogg E, et al. RAGE mediates amyloid-β peptide transport across the blood-brain barrier and accumulation in brain. Nat Med. 2003;9:907–13.
56. Majores M, Kölsch H, Bagli M, Ptok U, Kockler M, Becker K, et al. The insulin gene VNTR polymorphism in Alzheimer's disease: results of a pilot study. J Neural Transm. 2002;109:1029–34. doi:10.1007/s007020200086.
57. Kimura A, Hata S, Suzuki T. Alternative Selection of β-Site APP-Cleaving Enzyme 1 (BACE1) Cleavage Sites in Amyloid β-Protein Precursor (APP) Harboring Protective and Pathogenic Mutations within the Aβ Sequence. J Biol Chem. 2016;291:24041–53. doi:10.1074/jbc.M116.744722.
58. Fitz NF, Tapias V, Cronican AA, Castranio EL, Saleem M, Carter AY, et al. Opposing effects of *Apoe* / *Apoa1* double deletion on amyloid-β pathology and cognitive performance in APP mice. Brain. 2015;138:3699–715. doi:10.1093/brain/awv293.
59. Shinohara M, Tachibana M, Kanekiyo T, Bu G. Role of LRP1 in the pathogenesis of Alzheimer's disease: evidence from clinical and preclinical studies. J Lipid Res. 2017;58:1267–81. doi:10.1194/jlr.R075796.
60. Scacchi R, Gambina G, Moretto G, Corbo RM. Variability of AChE, BChE, and ChAT genes in the late-onset form of Alzheimer's disease and relationships with response to treatment with Donepezil and Rivastigmine. Am J Med Genet Part B Neuropsychiatr Genet. 2009;150B:502–7. doi:10.1002/ajmg.b.30846.
61. Jha NK, Jha SK, Kumar D, Kejriwal N, Sharma R, Ambasta RK, et al. Impact of Insulin Degrading Enzyme and Neprilysin in Alzheimer's Disease Biology: Characterization of Putative Cognates for Therapeutic Applications. J Alzheimer's Dis. 2015;48:891–917. doi:10.3233/JAD-150379.
62. Kang T, Qu Q, Xie Z, Cao B. NDRG4 Alleviates Aβ1–40 Induction of SH-SY5Y Cell Injury via Activation of BDNF-Inducing Signalling Pathways. Neurochem Res. 2020;45:1492–9. doi:10.1007/s11064-020-03011-4.

63. Akhtar A, Dhaliwal J, Saroj P, Uniyal A, Bishnoi M, Sah SP. Chromium picolinate attenuates cognitive deficit in ICV-STZ rat paradigm of sporadic Alzheimer's-like dementia via targeting neuroinflammatory and IRS-1/PI3K/AKT/GSK-3β pathway. Inflammopharmacology. 2020;28:385–400. doi:10.1007/s10787-019-00681-7.
64. Chahrour M, Sung YJ, Shaw C, Zhou X, Wong STC, Qin J, et al. MeCP2, a key contributor to neurological disease, activates and represses transcription. Science (80-). 2008;320:1224–9. doi:10.1126/science.1153252.
65. Burgos-Ramos E, Hervás-Aguilar A, Aguado-Llera D, Puebla-Jiménez L, Hernández-Pinto AM, Barrios V, et al. Somatostatin and Alzheimer's disease. Mol Cell Endocrinol. 2008;286:104–11.
66. Aguado-Llera D, Canelles S, Frago LM, Chowen JA, Argente J, Arilla E, et al. The Protective Effects of IGF-I against β-Amyloid-related Downregulation of Hippocampal Somatostatinergic System Involve Activation of Akt and Protein Kinase A. Neuroscience. 2018;374:104–18.
67. Sandoval K, Umbaugh D, House A, Crider A, Witt K. Somatostatin Receptor Subtype-4 Regulates mRNA Expression of Amyloid-Beta Degrading Enzymes and Microglia Mediators of Phagocytosis in Brains of 3xTg-AD Mice. Neurochem Res. 2019;44:2670–80. doi:10.1007/s11064-019-02890-6.
68. Saiz-Sanchez D, Ubeda-Bañon I, de la Rosa-Prieto C, Argandoña-Palacios L, Garcia-Muñozguren S, Insausti R, et al. Somatostatin, tau, and β-amyloid within the anterior olfactory nucleus in Alzheimer disease. Exp Neurol. 2010;223:347–50. doi:10.1016/j.expneurol.2009.06.010.
69. Beal MF, Mazurek MF, Tran VT, Chattha G, Bird ED, Martin JB. Reduced numbers of somatostatin receptors in the cerebral cortex in Alzheimer's disease. Science (80-). 1985;229:289–91.
70. Zhang S, Janciauskiene S. Multi-functional capability of proteins: α1-antichymotrypsin and the correlation with Alzheimer's disease. J Alzheimer's Dis. 2002;4:115–22.
71. Abraham CR, Potter H. The protease inhibitor, α1-antichymotrypsin, is a component of the brain amyloid deposits in normal aging and Alzheimer's disease. Ann Med. 1989;21:77–81.
72. Eriksson S, Janciauskiene S, Lannfelt L. α1-Antichymotrypsin regulates Alzheimer β-amyloid peptide fibril formation. Proc Natl Acad Sci U S A. 1995;92:2313–7.
73. Tyagi E, Fiorelli T, Norden M, Padmanabhan J. Alpha 1-antichymotrypsin, an inflammatory protein overexpressed in the brains of patients with Alzheimer's disease, induces Tau hyperphosphorylation through c-Jun N-terminal kinase activation. Int J Alzheimers Dis. 2013;2013:1–12.
74. Padmanabhan J, Levy M, Dickson DW, Potter H. Alpha1-antichymotrypsin, an inflammatory protein overexpressed in Alzheimer's disease brain, induces tau phosphorylation in neurons. Brain. 2006;129:3020–34.
75. Kume H, Konishi Y, Murayama KS, Kametani F, Araki W. Expression of reticulon 3 in Alzheimer's disease brain. Neuropathol Appl Neurobiol. 2009;35:178–88.
76. He W, Hu X, Shi Q, Zhou X, Lu Y, Fisher C, et al. Mapping of Interaction Domains Mediating Binding between BACE1 and RTN/Nogo Proteins. J Mol Biol. 2006;363:625–34.
77. He W, Shi Q, Hu X, Yan R. The membrane topology of RTN3 and its effect on binding of RTN3 to BACE1. J Biol Chem. 2007;282:29144–51.
78. Sharoar MG, Yan R. Effects of altered RTN3 expression on BACE1 activity and Alzheimer's neuritic plaques. Rev Neurosci. 2017;28:145–54.
79. He W, Lu Y, Qahwash I, Hu XY, Chang A, Yan R. Reticulon family members modulate BACE1 activity and amyloid-β peptide generation. Nat Med. 2004;10:959–65.

80. Wang T, Chen J, Hou Y, Yu Y, Wang B. BAP31 deficiency contributes to the formation of amyloid-b plaques in Alzheimer's disease by reducing the stability of RTN3. FASEB J. 2019;33:4936–46.
81. Emilsson L. Detection of Differentially Expressed Genes in Alzheimer's Disease. Uppsala University; 2005.

Figures

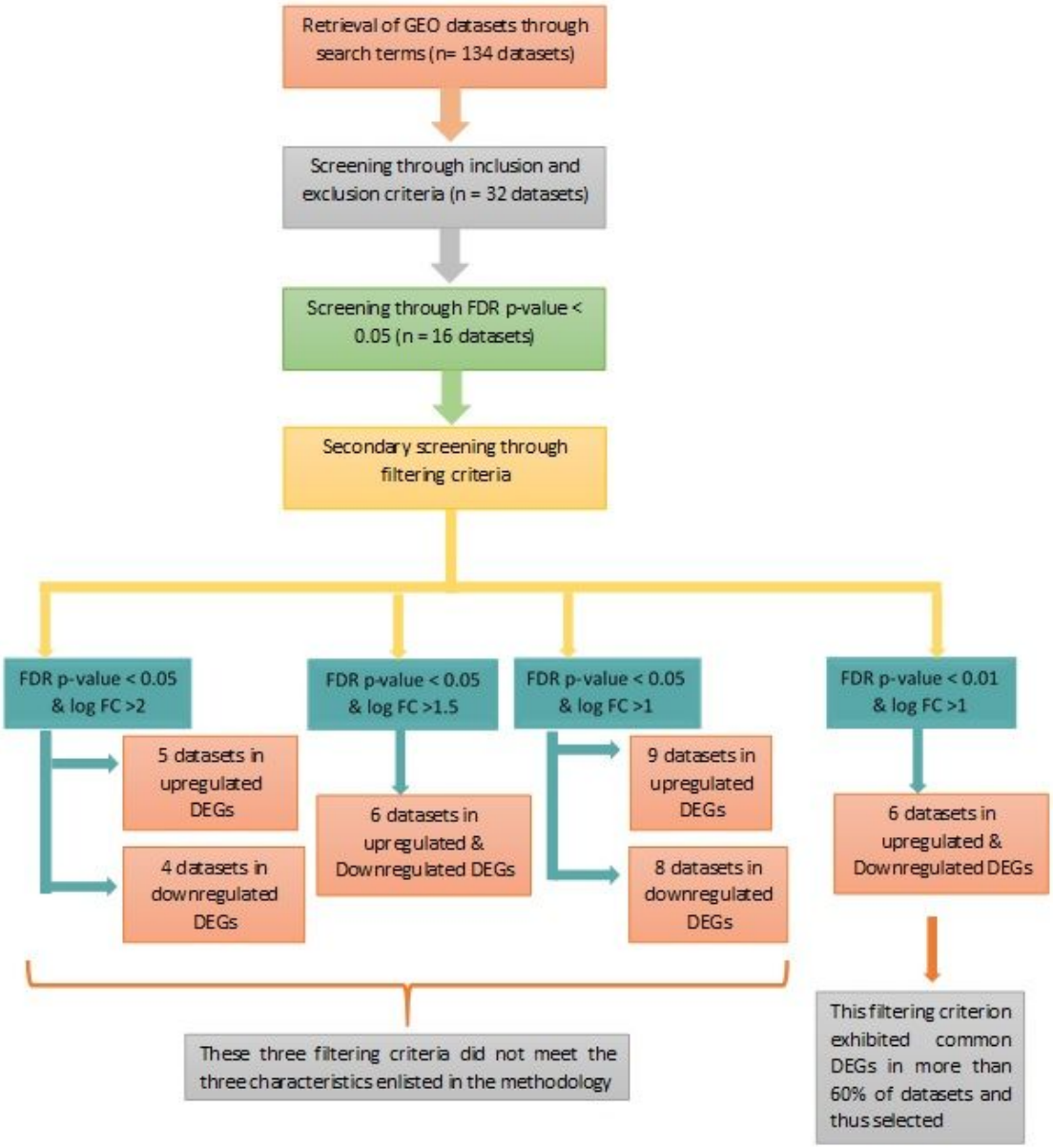

Figure 1

Consort explaining the selection and screening of datasets

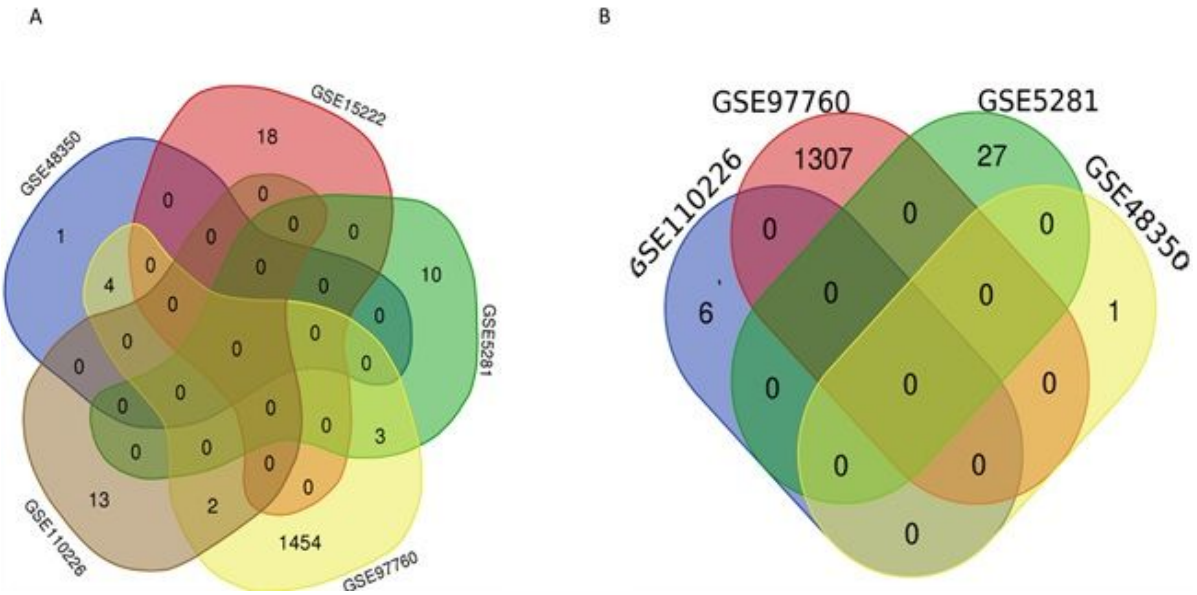

Figure 2

Venn Diagram exhibiting the common upregulated (A) and downregulated (B) DEGs

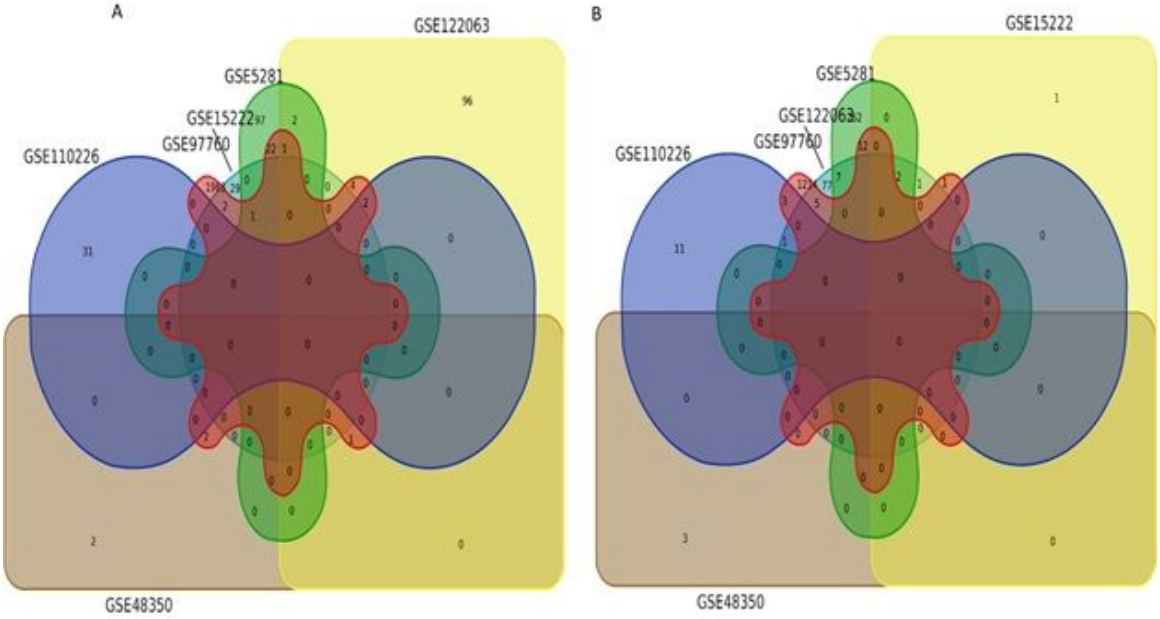

Figure 3

Venn Diagram exhibiting the common upregulated (A) and downregulated (B) DEGs

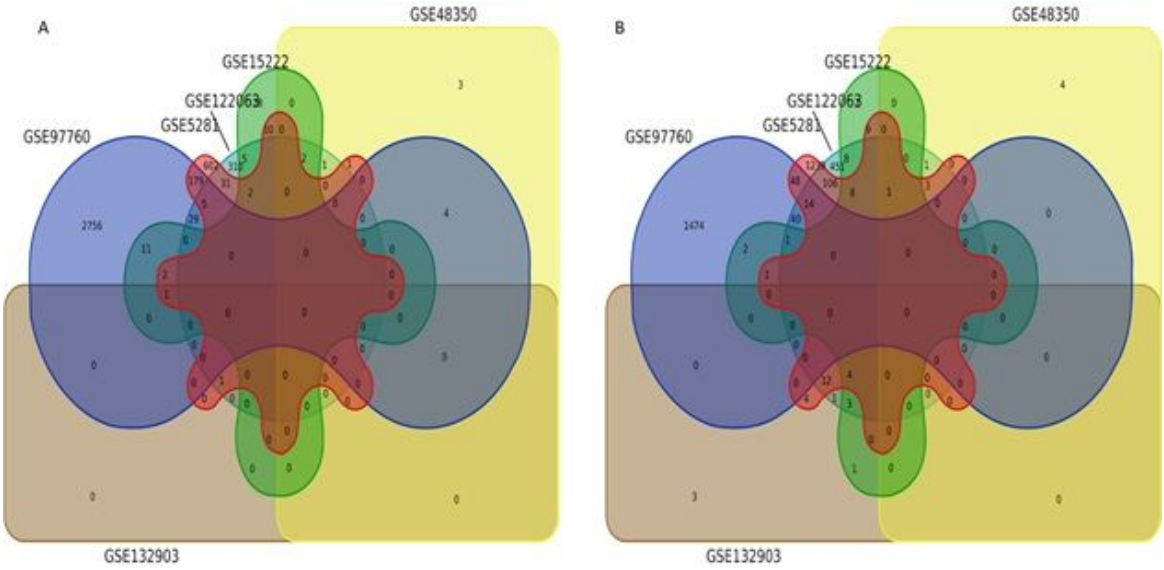

Figure 4

Venn Diagram exhibiting the common upregulated (A) and downregulated (B) DEGs

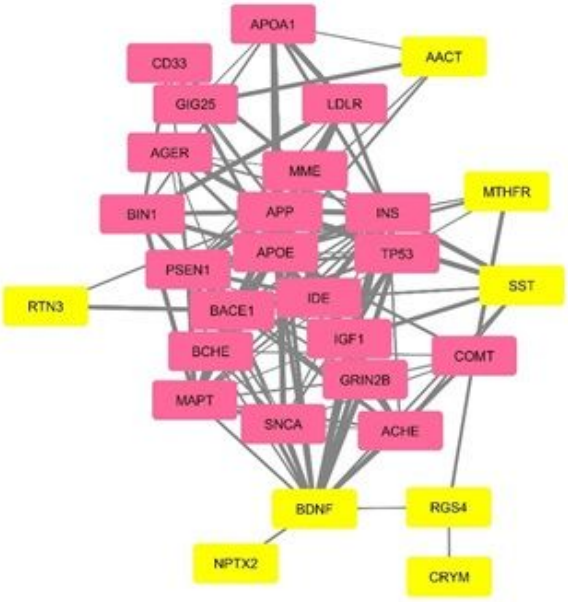

Figure 5

PPI network exhibiting significant interactions with LDGs. Yellow nodes represent common genes retrieved from GEO datasets. Pink nodes represent LDGs.

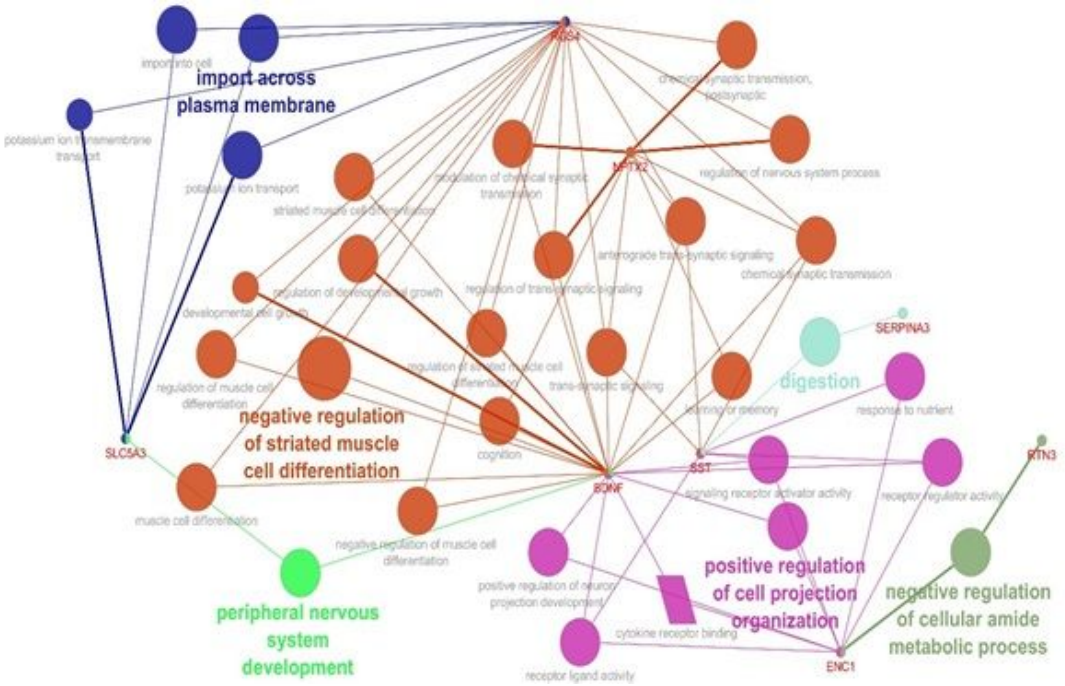

Figure 6

Gene ontology categories of common DEGs describing their physiological roles

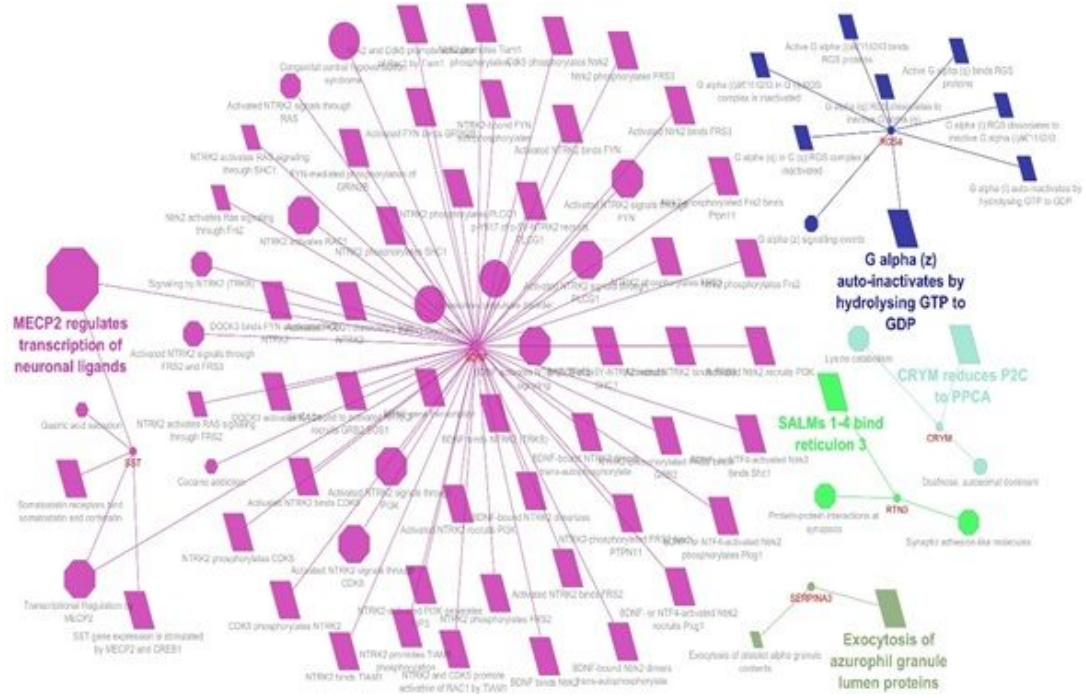

Figure 7

Significant KEGG pathways of common DEGs

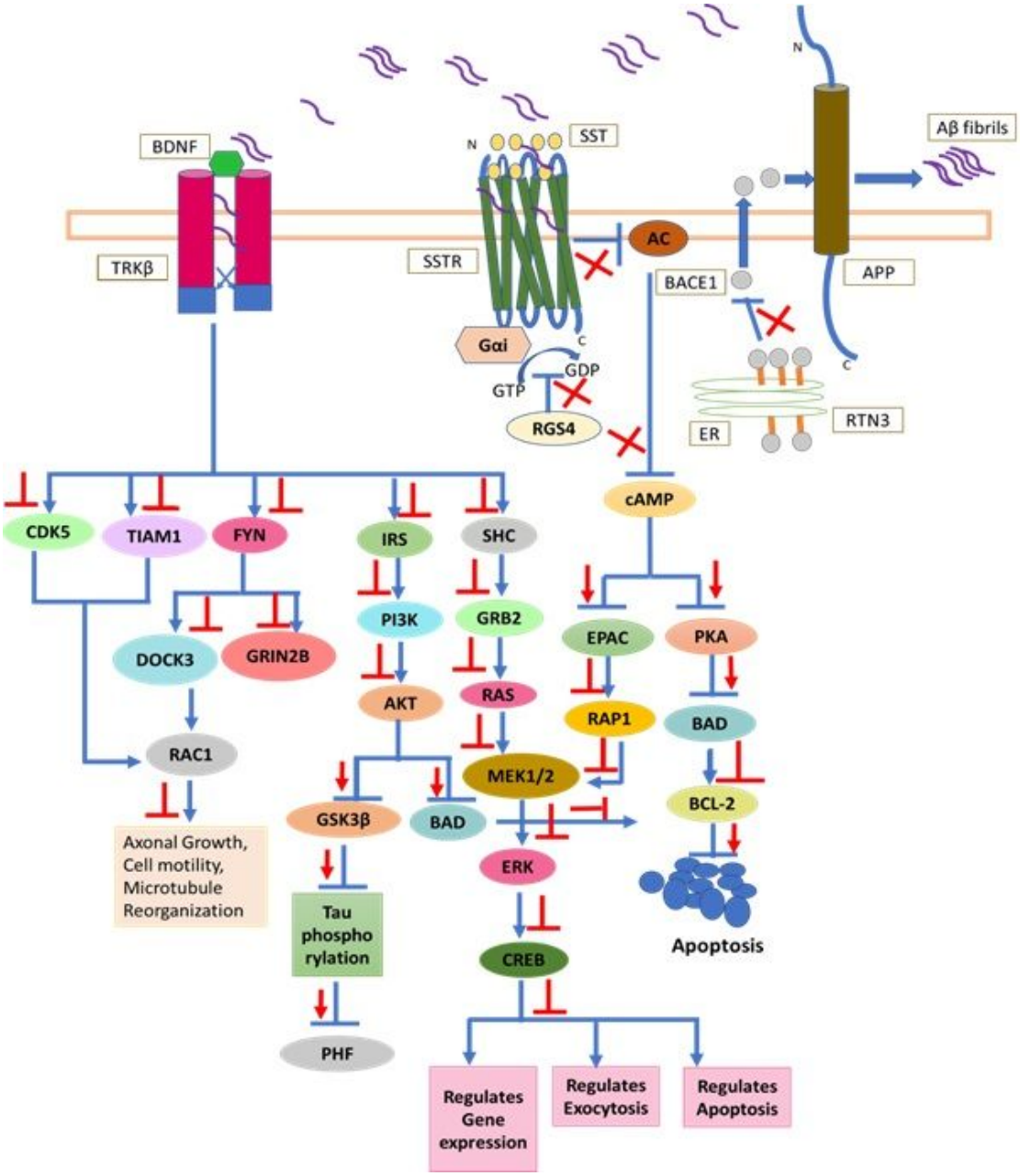

Figure 8

Various signalling mechanisms and crosstalks underlying the AD progression. Blue coloured arrows represent signalling mechanisms in the absence of Aβ fibrils and red coloured arrows represent signalling responses in the presence of Aβ fibrils. BDNF: Brain Derived Neurotrophic Factor, TRKβ: Tyrosine Kinase β, SST: Somatostatin, SSTR: Somatostatin Receptor, APP: Amyloid Precursor Protein, AC Adenyl Cyclase, BACE1: Beta-Secretase 1, ER: Endoplasmic Reticulum, RTN3: Reticulon 3, GTP: Guanine Tri Phosphate, GDP: Guanine Di Phosphate, RGS4: Regulator of G Protein Signalling 4, cAMP: cyclic Adenosine Mono Phosphate, CDK5: Cyclin Dependent Kinase 5, TIAM1: T-Lymphoma Invasion And Metastasis-Inducing Protein 1, FYN: Fyn kinase, IRS: Insulin Receptor Substrate, SHC: T-Lymphoma Invasion And Metastasis-Inducing Protein 1, DOCK3: Dedicator Of Cytokinesis 3, GRIN2B: Glutamate Ionotropic Receptor NMDA Type Subunit 2B, RAC1: Rac Family Small GTPase 1, PI3K: Phosphatidylinositol-4,5-Bisphosphate 3-Kinase, AKT: AKT Serine/Threonine Kinase , GSK3β: Glycogen Synthase Kinase 3β, BAD: BCL2 Associated Agonist Of Cell Death, GRB2: Growth Factor Receptor Bound Protein 2, RAS: KRAS Proto-Oncogene, GTPase, MEK: Mitogen-Activated Protein Kinase, ERK: Extracellular signal Related Kinase,

CREB: CAMP Responsive Element Binding Protein 1, PHF: Paired Helical Filaments, EPAC: Rap Guanine Nucleotide Exchange Factor 3, RAP1: Member Of RAS Oncogene Family, PKA: Protein Kinase A, BCL2: BCL2 Apoptosis Regulator